R

The Mathematics of Finite Rotations

TABLE OF CONTENTS

This Appendix collects formulas and results for the mathematical treatment of finite rotations in 3D space. Emphasis is placed on representations useful in the CR description of FEM. Several of the results are either new or simplifications of published results. Some statements in the literature concerning the exponential and Cayley maps are shown to be erroneous.

One difficulty for investigators and students learning the CR description is that different normalizations have been used by different authors. This topic is reviewed in some detail, and summary help provided in the form of Table R.5.

§R.1. Spatial Rotations

Plane rotations are easy. A rotation in, say, the $\{x_1, x_2\}$ plane, is defined by just a scalar: the rotation angle θ about x_3. Plane rotations commute: $\theta_1 + \theta_2 = \theta_2 + \theta_1$, because the θs are numbers.

The study of spatial (3D) rotations is more difficult. The subject is dominated by a fundamental theorem of Euler:

> *The general displacement of a rigid body with one point fixed is a rotation about some axis which passes through that point.* (R.1)

Thus spatial rotations have both magnitude: the angle of rotation, and direction: the axis of rotation. These are nominally the same two attributes that categorize vectors. Not coincidentally, rotations are sometimes pictured as vectors but with a double arrow in Mechanics books. Finite 3D rotations, however, do not obey the laws of vector calculus, although infinitesimal rotations do. Most striking is commutation failure: switching two successive rotations does not yield the same answer unless the rotation axis is kept fixed. Within the framework of matrix algebra, finite rotations can be represented in two ways:

(a) As 3×3 real orthogonal matrices $\mathbf{R}$ called *rotators*. (An abbreviation for *rotation tensor*).

(b) As 3×3 real skew-symmetric matrices $\mathbf{\Omega}$ called *spinors*. (An abbreviation for *spin tensor*).

The spinor representation is important in theory and modeling because the matrix entries are closely related to the ingredients of Euler's theorem (R.1).

The rotator representation is convenient for numerical work, as well as being naturally related to the polar factorization of a transformation matrix. The two representations are connected as illustrated in Figure R.1, which also includes the axial vector introduced below. Of the $\mathbf{\Omega} \to \mathbf{R}$ links, the Rodrigues-Cayley version is historically the first, as discussed in [R.20], although not the most important one.

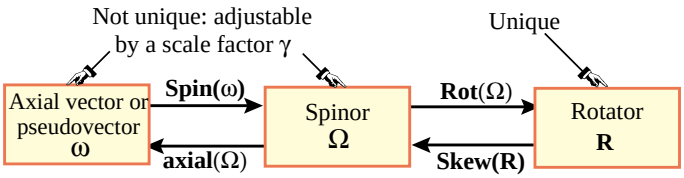

FIGURE R.1. Representations of finite spatial rotations. Note: Some authors write $e^{\mathbf{\Omega}}$ and $\mathbf{Log}_e(\mathbf{R})$ for $\mathbf{Rot}(\mathbf{\Omega})$ and $\mathbf{Skew}(\mathbf{R})$, respectively. This is correct for a particular scale factor γ; cf. Table R.5.

A 3×3 skew-symmetric matrix such as $\mathbf{\Omega}$ is defined by three scalar parameters. These three numbers can be arranged as components of an *axial vector* $\boldsymbol{\omega}$. Although $\boldsymbol{\omega}$ looks like a 3-vector, it violates certain properties of classical vectors such as the composition rule. Therefore the term *pseudovector* is sometimes used for $\boldsymbol{\omega}$.

In the EICR formulation presented here, axial vectors of rotations and spins function as incremental quantities directly connected to variations. Rotator matrices are used to record the global structure motions. See Table R.2.

This Appendix intends to convey that finite 3D rotations can appear in alternative mathematical representations, as diagramed in Figure R.1. The following exposition expands on this topic, and studies the links shown there.

§R.2. Spinors

Figure R.2(a) depicts a 3D rotation in space $\{x_1, x_2, x_3\}$ by an angle θ about an axis of rotation $\vec{\boldsymbol{\omega}}$. For convenience the origin of coordinates O is placed on $\vec{\boldsymbol{\omega}}$. The rotation axis is defined by three directors: $\omega_1, \omega_2, \omega_3$, at least one of which must be nonzero. These components may be scaled by an nonzero factor γ through which the vector may be normalized in various ways discussed later. The rotation takes an arbitrary point $P(\mathbf{x})$, located by its position vector $\mathbf{x}$, into $Q(\mathbf{x}, \theta)$, located by its position vector $\mathbf{x}_\theta$. The center of rotation C is defined by projecting P on the rotation axis. The plane of rotation CPQ is normal to that axis at C.

The radius of rotation is vector **r** of magnitude r from C to P. As illustrated in Figure R.2(b) the distance between P and Q is $2r \sin \frac{1}{2}\theta$.

The positive sense of θ obeys the RHS screw rule: positive counterclockwise if observed from the tip of the rotation axis. The angle shown in Figure R.2 is positive.

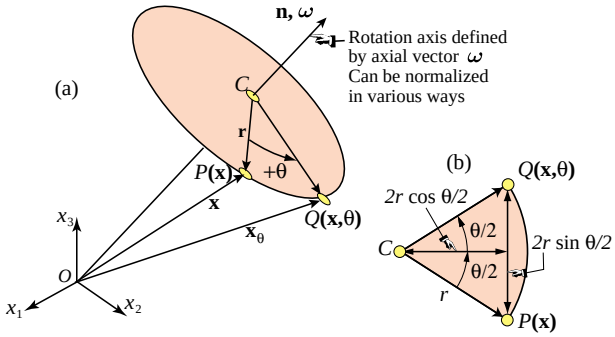

FIGURE R.2. The rotation angle θ is positive as shown, obeying the right-hand screw rule about the rotation axis.

§R.3. Spin Tensor and Axial Vector

Given the three directors ω_1, ω_2, and ω_3 of the axis $\boldsymbol{\omega}$, we can associate with it a 3×3 skew-symmetric matrix $\boldsymbol{\Omega}$, called a *spin tensor*, *spin matrix* or briefly *spinor*, by the rule

$$\boldsymbol{\Omega} = \mathbf{Spin}(\boldsymbol{\omega}) = \begin{bmatrix} 0 & -\omega_3 & \omega_2 \\ \omega_3 & 0 & -\omega_1 \\ -\omega_2 & \omega_3 & 0 \end{bmatrix} = -\boldsymbol{\Omega}^T. \tag{R.2}$$

The space of all $\boldsymbol{\Omega}$'s form the Lie algebra $so(3)$. Premultiplication of an arbitrary 3-vector **v** by $\boldsymbol{\Omega}$ is equivalent to the cross product of $\boldsymbol{\omega}$ and **v**:

$$\boldsymbol{\omega} \times \mathbf{v} = \boldsymbol{\Omega}\,\mathbf{v} = \mathbf{Spin}(\boldsymbol{\omega})\,\mathbf{v} = -\mathbf{Spin}(\mathbf{v})\,\boldsymbol{\omega} = -\mathbf{v} \times \boldsymbol{\omega}. \tag{R.3}$$

In particular $\boldsymbol{\Omega}\,\boldsymbol{\omega} = \mathbf{0}$, and $\mathbf{v}^T\boldsymbol{\Omega}\,\mathbf{v} = 0$, as may be directly verified. The operation converse to (R.2) extracts the 3-vector $\boldsymbol{\omega}$, called *axial vector* or *pseudovector*, from a given spin tensor:

$$\boldsymbol{\omega} = \mathbf{axial}(\boldsymbol{\Omega}) = \begin{bmatrix} \omega_1 \\ \omega_2 \\ \omega_3 \end{bmatrix} \tag{R.4}$$

The length of this vector is denoted by ω:

$$\omega = |\boldsymbol{\omega}| = +\sqrt{\omega_1^2 + \omega_2^2 + \omega_3^2}. \tag{R.5}$$

As general notational rule, we will use corresponding upper and lower case symbols for the spinor and its axial vector, respectively, if possible. For example, **N** and **n**, $\boldsymbol{\Theta}$ and $\boldsymbol{\theta}$, **V** and **v**. Exceptions are made in case of notational conflicts; for example the spinor built from the quaternion vector p_i is not denoted as **P** because that symbol is reserved for projectors.

§R.4. Spinor Normalizations

As noted, $\boldsymbol{\omega}$ and $\boldsymbol{\Omega}$ can be multiplied by a nonzero scalar factor γ to obtain various *normalizations*. In general γ has the form $g(\theta)/\omega$, where $g(.)$ is a function of the rotation angle θ. The goal of normalization is to simplify the connections **Rot** and **Skew** to the rotator, to avoid singularities for special angles, and to connect the components ω_1, ω_2 and ω_3 closely to the rotation amplitude. This section overviews some normalizations that have practical or historical importance.

Choosing $\gamma = 1/\omega$ we obtain the unit axial-vector and unit spinor, which are denoted by **n** and **N**, respectively:

$$\mathbf{n} = \begin{bmatrix} n_1 \\ n_2 \\ n_3 \end{bmatrix} = \begin{bmatrix} \omega_1/\omega \\ \omega_2/\omega \\ \omega_3/\omega \end{bmatrix} = \frac{\boldsymbol{\omega}}{\omega}, \quad \mathbf{N} = \mathbf{Spin}(\mathbf{n}) = \frac{\boldsymbol{\Omega}}{\omega} = \begin{bmatrix} 0 & -n_3 & n_2 \\ n_3 & 0 & -n_1 \\ -n_2 & n_3 & 0 \end{bmatrix}. \tag{R.6}$$

Taking $\gamma = \tan\frac{1}{2}\theta/\omega$ is equivalent to multiplying the n_i by $\tan\frac{1}{2}\theta$. We thus obtain the parameters $b_i = n_i \tan\frac{1}{2}\theta$, $i = 1, 2, 3$ attributed to Rodrigues [R.69] by Cheng and Gupta [R.20]. These are collected in the Rodrigues axial-vector **b** with associated spinor $\boldsymbol{\mathcal{Z}}$:

$$\mathbf{b} = \tan\tfrac{1}{2}\theta\,\mathbf{n} = (\tan\tfrac{1}{2}\theta/\omega)\,\boldsymbol{\omega}, \quad \boldsymbol{\mathcal{Z}} = \mathbf{Spin}(\mathbf{b}) = \tan\tfrac{1}{2}\theta\,\mathbf{N} = (\tan\tfrac{1}{2}\theta/\omega)\,\boldsymbol{\Omega}. \tag{R.7}$$

This representation permits an elegant formulation of the rotator via the Cayley transform studied later. However, it collapses as θ nears $\pm 180^\circ$ since $\tan \frac{1}{2}\theta \to \pm\infty$. One way to circumvent the singularity is through the use of the four Euler-Rodrigues parameters, also called *quaternion coefficients*:

$$p_0 = \cos \tfrac{1}{2}\theta, \quad p_i = n_i \sin \tfrac{1}{2}\theta = \omega_i/\omega \sin \tfrac{1}{2}\theta, \quad i = 1, 2, 3. \tag{R.8}$$

under the constraint $p_0^2 + p_1^2 + p_2^2 + p_3^2 = 1$. This set is often used in multibody dynamics, robotics and control. It comes at the cost of carrying along an extra parameter and an additional constraint.

A related singularity-free normalization introduced by Fraeijs de Veubeke [R.25] takes $\gamma = \sin \frac{1}{2}\theta/\omega$ and is equivalent to using only the last three parameters of (R.8):

$$\mathbf{p} = \sin \tfrac{1}{2}\theta\, \mathbf{n} = (\sin \tfrac{1}{2}\theta/\omega)\ \boldsymbol{\omega}, \quad \boldsymbol{\Omega}_p = \mathbf{Spin}(\mathbf{p}) = \sin \tfrac{1}{2}\theta\, \mathbf{N} = (\sin \tfrac{1}{2}\theta/\omega)\ \boldsymbol{\Omega}. \tag{R.9}$$

Fraeijs de Veubeke calls this representation "Rodrigues-Hamilton" without explanatory references.

Finally, an important normalization that preserves three parameters while avoiding singularities is that associated with the exponential map. Introduce a *rotation vector* $\boldsymbol{\theta}$ defined as

$$\boldsymbol{\theta} = \theta \mathbf{n} = (\theta/\omega)\, \boldsymbol{\omega}, \quad \boldsymbol{\Theta} = \mathbf{Spin}(\boldsymbol{\theta}) = \theta\, \mathbf{N} = (\theta/\omega)\, \boldsymbol{\Omega}. \tag{R.10}$$

For this normalization the angle is the length of the rotation vector: $\theta = |\boldsymbol{\theta}| = \sqrt{\theta_1^2 + \theta_2^2 + \theta_3^2}$. The selection of the sign of θ is a matter of convention.

§R.5. Spectral Properties

The study of the spinor eigensystem $\boldsymbol{\Omega}\, \mathbf{z}_i = \lambda_i \mathbf{z}_i$ is of interest for various developments. Begin by forming the characteristic equation

$$\det(\boldsymbol{\Omega} - \lambda \mathbf{I}) = -\boldsymbol{\lambda}^3 - \omega^2 \lambda = 0 \tag{R.11}$$

where $\mathbf{I}$ denotes the identity matrix of order 3. It follows that the eigenvalues of $\boldsymbol{\Omega}$ are $\lambda_1 = 0$, $\lambda_{2,3} = \pm \omega i$. Consequently $\boldsymbol{\Omega}$ is singular with rank 2 if $\omega \neq 0$, whereas if $\omega = 0$, $\boldsymbol{\Omega}$ is null.

The eigenvalues are collected in the diagonal matrix $\boldsymbol{\Lambda} = \mathbf{diag}(0,\ \omega i,\ -\omega i)$ and the corresponding right eigenvectors $\mathbf{z}_i$ in columns of $\mathbf{Z} = [\, \mathbf{z}_1\ \ \mathbf{z}_2\ \ \mathbf{z}_3\,]$, so that $\boldsymbol{\Omega}\, \mathbf{Z} = \mathbf{Z}\boldsymbol{\Lambda}$. A cyclic-symmetric expression of $\mathbf{Z}$, obtained through *Mathematica*, is

$$\mathbf{Z} = \begin{bmatrix} \omega_1 & \omega_1 s - \omega^2 + i(\omega_2 - \omega_3)\omega & \omega_1 s - \omega^2 - i(\omega_2 - \omega_3)\omega \\ \omega_2 & \omega_2 s - \omega^2 + i(\omega_3 - \omega_1)\omega & \omega_2 s - \omega^2 - i(\omega_3 - \omega_1)\omega \\ \omega_3 & \omega_3 s - \omega^2 + i(\omega_1 - \omega_2)\omega & \omega_3 s - \omega^2 - i(\omega_1 - \omega_2)\omega \end{bmatrix} \tag{R.12}$$

where $s = \omega_1 + \omega_2 + \omega_3$. Its inverse is

$$\mathbf{Z}^{-1} = \frac{1}{\omega^2} \begin{bmatrix} \omega_1 & -\frac{1}{2}\dfrac{\omega_2^2 + \omega_3^2}{\omega_1 s - \omega^2 - i(\omega_2 - \omega_3)\omega} & -\frac{1}{2}\dfrac{\omega_2^2 + \omega_3^2}{\omega_1 s - \omega^2 + i(\omega_2 - \omega_3)\omega} \\ \omega_2 & -\frac{1}{2}\dfrac{\omega_3^2 + \omega_1^2}{\omega_2 s - \omega^2 - i(\omega_3 - \omega_1)\omega} & -\frac{1}{2}\dfrac{\omega_3^2 + \omega_1^2}{\omega_2 s - \omega^2 + i(\omega_3 - \omega_1)\omega} \\ \omega_3 & -\frac{1}{2}\dfrac{\omega_1^2 + \omega_2^2}{\omega_3 s - \omega^2 - i(\omega_1 - \omega_2)\omega} & -\frac{1}{2}\dfrac{\omega_1^2 + \omega_2^2}{\omega_3 s - \omega^2 + i(\omega_1 - \omega_2)\omega} \end{bmatrix} \tag{R.13}$$

The real and imaginary part of the eigenvectors $\mathbf{z}_2$ and $\mathbf{z}_3$ are orthogonal. This is a general property of skew-symmetric matrices; cf. Bellman [R.6, p. 64]. Because the eigenvalues of $\boldsymbol{\Omega}$ are distinct if $\omega \neq 0$, an arbitrary matrix function $\mathbf{F}(\boldsymbol{\Omega})$ can be explicitly obtained as

$$\mathbf{F}(\boldsymbol{\Omega}) = \mathbf{Z} \begin{bmatrix} f(0) & 0 & 0 \\ 0 & f(\omega i) & 0 \\ 0 & 0 & f(-\omega i) \end{bmatrix} \mathbf{Z}^{-1}, \tag{R.14}$$

where $f(.)$ denotes the scalar version of $\mathbf{F}(.)$. One important application of (R.14) is the matrix exponential, for which $f(.) \to e^{(.)}$.

The square of $\mathbf{\Omega}$, computed through direct multiplication, is

$$\mathbf{\Omega}^2 = -\begin{bmatrix} \omega_2^2+\omega_3^2 & -\omega_1\omega_2 & -\omega_1\omega_3 \\ -\omega_1\omega_2 & \omega_3^2+\omega_1^2 & -\omega_2\omega_3 \\ -\omega_1\omega_3 & -\omega_2\omega_3 & \omega_1^2+\omega_2^2 \end{bmatrix} = \boldsymbol{\omega}\boldsymbol{\omega}^T - \omega^2\mathbf{I} = \omega^2(\mathbf{n}\mathbf{n}^T - \mathbf{I}). \tag{R.15}$$

This is a symmetric matrix of trace $-2\omega^2$ whose eigenvalues are 0, $-\omega^2$ and $-\omega^2$. By the Cayley-Hamilton theorem, $\mathbf{\Omega}$ satisfies its own characteristic equation (R.11):

$$\mathbf{\Omega}^3 = -\omega^2\mathbf{\Omega}, \quad \mathbf{\Omega}^4 = -\omega^2\mathbf{\Omega}^2, \ \ldots \quad \text{and generally} \quad \mathbf{\Omega}^n = -\omega^2\mathbf{\Omega}^{n-2}, \ n \ge 3. \tag{R.16}$$

Hence if $n = 3, 5, \ldots$ the odd powers $\mathbf{\Omega}^n$ are skew-symmetric with distinct purely imaginary eigenvalues, whereas if $n = 4, 6 \ldots$, the even powers $\mathbf{\Omega}^n$ are symmetric with repeated real eigenvalues.

The eigenvalues of $\mathbf{I}+\gamma\mathbf{\Omega}$ and $\mathbf{I}-\gamma\mathbf{\Omega}$, are $(1, 1\pm\gamma\omega i)$ and $(-1, 1\pm\gamma\omega i)$, respectively. Hence those two matrices are guaranteed to be nonsingular. This has implications in the Cayley transform (R.29).

Example. Consider the pseudo-vector $\boldsymbol{\omega} = [\,6 \quad 2 \quad 3\,]^T$, for which $\omega = \sqrt{6^2+2^2+3^2} = 7$. The associated spin matrix and its square are

$$\mathbf{\Omega} = \begin{bmatrix} 0 & -3 & 2 \\ 3 & 0 & -6 \\ -2 & 6 & 0 \end{bmatrix}, \quad \mathbf{\Omega}^2 = -\begin{bmatrix} 13 & -12 & -18 \\ -12 & 45 & -6 \\ -18 & -6 & 40 \end{bmatrix}, \quad \mathbf{\Omega}^3 = -49\,\mathbf{\Omega}, \ldots \tag{R.17}$$

The eigenvalues of $\mathbf{\Omega}$ are $(0, 7i, -7i)$ while those of $\mathbf{\Omega}^2$ are $(0, -7, -7)$.

§R.6. From Spinors To Rotators

Referring to Figure R.2, a rotator is a linear operator that maps a generic point $P(\mathbf{x})$ to $Q(\mathbf{x}_\theta)$ given the rotation axis $\vec{\omega}$ and the angle θ. We consider only rotator representations in the form of 3×3 *rotation matrices* $\mathbf{R}$, defined by

$$\mathbf{x}_\theta = \mathbf{R}\,\mathbf{x}, \qquad \mathbf{x} = \mathbf{R}^T\mathbf{x}_\theta. \tag{R.18}$$

The rotation matrix is *proper orthogonal*, that is, $\mathbf{R}^T\mathbf{R} = \mathbf{I}$ and $\det(\mathbf{R}) = +1$. It must reduce to $\mathbf{I}$ if the rotation vanishes. The space of all $\mathbf{R}$s form the rotation group SO(3).

Remark 5. The definition (R.18) is taken to agree with the convention for positive rotation angle θ illustrated in Figure R.2 and the definition of $\mathbf{Spin}(\boldsymbol{\omega})$ given in (R.2). Several books, e.g. Goldstein [R.35], define as spin matrix $\mathbf{\Omega}$ the transpose of ours. The definition used here agrees with that of the historical review article by Cheng and Gupta [R.20]. Readers consulting the literature or implementing finite rotation analysis are advised to check sign conventions carefully. A recommended verification is to work out the 2D case by hand, since the specialization to plane rotation should produce well known coordinate transformations.

§R.7. Rotator Parametrizations

A key attribute of $\mathbf{R}$ is the *trace property*

$$\mathbf{trace}(\mathbf{R}) = 1 + 2\cos\theta, \tag{R.19}$$

proofs of which may be found for example in Goldstein [R.35, p. 123] or Hammermesh [R.36, p. 326]. (It follows from the fact that the eigenvalues of $\mathbf{R}$ are 1, $e^{\theta i}$ and $e^{-\theta i}$ and their sum is (R.19).) The problem considered here is the construction of $\mathbf{R}$ from rotation data. The inverse problem: given $\mathbf{R}$, extract spin and/or rotation angles, is treated later. Now if $\mathbf{R}$ is assumed to be analytic in $\mathbf{\Omega}$ it must have the Taylor expansion $\mathbf{R} = \mathbf{I} + c_1\mathbf{\Omega} + c_2\mathbf{\Omega}^2 + c_3\mathbf{\Omega}^3 + \ldots$, where all c_i must vanish if $\theta = 0$. But because of the Cayley-Hamilton theorem (R.16), all powers of order 3 or higher may be eliminated. Thus $\mathbf{R}$ must be a linear function of $\mathbf{I}$, $\mathbf{\Omega}$ and $\mathbf{\Omega}^2$. For convenience this will be written

$$\mathbf{R} = \mathbf{I} + \alpha(\gamma\mathbf{\Omega}) + \beta(\gamma\mathbf{\Omega})^2. \tag{R.20}$$

Here γ is the spinor normalization factor whereas α and β are scalar functions of θ and of invariants of $\mathbf{\Omega}$ or $\boldsymbol{\omega}$. Since the only invariant of the latter is ω we may anticipate that $\alpha = \alpha(\theta, \omega)$ and $\beta = \beta(\theta, \omega)$, both vanishing if $\theta = 0$. Two techniques to determine those coefficients for $\gamma = 1$ are discussed in the next subsections. Table R.5 collects several representations of a rotator in terms of the scaled $\mathbf{\Omega}$, used by different authors.

Table R.5. Rotator Forms for Several Spinor Normalizations

Parametrization	γ	α	β	Spinor	Rotator $\mathbf{R}$
None (unscaled)	1	$\frac{\sin\theta}{\omega}$	$\frac{2\sin^2\frac{1}{2}\theta}{\omega^2}$	$\boldsymbol{\Omega}$	$\mathbf{I}+\frac{\sin\theta}{\omega}\boldsymbol{\Omega}+\frac{2\sin^2\frac{1}{2}\theta}{\omega^2}\boldsymbol{\Omega}^2$
Unit axial-vector	$\frac{1}{\omega}$	$\sin\theta$	$2\sin^2\frac{1}{2}\theta$	$\mathbf{N}=\gamma\boldsymbol{\Omega}$	$\mathbf{I}+\sin\theta\,\mathbf{N}+2\sin^2\frac{1}{2}\theta\,\mathbf{N}^2$,
Rodrigues-Cayley	$\frac{\tan\frac{1}{2}\theta}{\omega}$	$2\cos^2\frac{1}{2}\theta$	$2\cos^2\frac{1}{2}\theta$	$\boldsymbol{\Sigma}=\gamma\boldsymbol{\Omega}$	$\mathbf{I}+2\cos^2\frac{1}{2}\theta\,(\boldsymbol{\Sigma}+\boldsymbol{\Sigma}^2)=(\mathbf{I}+\boldsymbol{\Sigma})(\mathbf{I}-\boldsymbol{\Sigma})^{-1}$
Fraeijs de Veubeke	$\frac{\sin\frac{1}{2}\theta}{\omega}$	$2\cos\frac{1}{2}\theta$	2	$\boldsymbol{\Omega}_p=\gamma\boldsymbol{\Omega}$	$\mathbf{I}+2\cos\frac{1}{2}\theta\,\boldsymbol{\Omega}_p+2\boldsymbol{\Omega}_p^2$
Exponential map	$\frac{\theta}{\omega}$	$\frac{\sin\theta}{\theta}$	$\frac{2\sin^2\frac{1}{2}\theta}{\theta^2}$	$\boldsymbol{\Theta}=\gamma\boldsymbol{\Omega}$	$\mathbf{I}+\frac{\sin\theta}{\theta}\boldsymbol{\Theta}+\frac{2\sin^2\frac{1}{2}\theta}{\theta^2}\boldsymbol{\Theta}^2=e^{\boldsymbol{\Theta}}=e^{\theta\mathbf{N}}$

§R.7.1. Rotator From Algebra

It is possible to find α and β for $\gamma=1$ (the unscaled spinor) directly from algebraic conditions. Taking the trace of (R.20) for $\gamma=1$ and applying the property (R.19) requires

$$3-2\beta\omega^2=1+2\cos\theta,\quad\text{whence}\quad\beta=\frac{1-\cos\theta}{\omega^2}=\frac{2\sin^2\frac{1}{2}\theta}{\omega^2}. \tag{R.21}$$

The orthogonality condition $\mathbf{I}=\mathbf{R}^T\mathbf{R}=(\mathbf{I}-\alpha\boldsymbol{\Omega}+\beta\boldsymbol{\Omega}^2)(\mathbf{I}+\alpha\boldsymbol{\Omega}+\beta\boldsymbol{\Omega}^2)=\mathbf{I}+(2\beta-\alpha^2)\boldsymbol{\Omega}^2+\beta^2\boldsymbol{\Omega}^4=\mathbf{I}+(2\beta-\alpha^2-\beta^2\omega^2)\boldsymbol{\Omega}^2$ leads to

$$2\beta-\alpha^2-\beta^2\omega^2=0,\quad\text{whence}\quad\alpha=\frac{\sin\theta}{\omega}. \tag{R.22}$$

Therefore

$$\mathbf{R}=\mathbf{I}+\frac{\sin\theta}{\omega}\boldsymbol{\Omega}+\frac{1-\cos\theta}{\omega^2}\boldsymbol{\Omega}^2=\mathbf{I}+\frac{\sin\theta}{\omega}\boldsymbol{\Omega}+\frac{2\sin^2\frac{1}{2}\theta}{\omega^2}\boldsymbol{\Omega}^2. \tag{R.23}$$

From a numerical standpoint the sine-squared form should be preferred to avoid the cancellation in computing $1-\cos\theta$ for small θ. Replacing the components of $\boldsymbol{\Omega}$ and $\boldsymbol{\Omega}^2$ gives the explicit rotator form

$$\mathbf{R}=\frac{1}{\omega^2}\begin{bmatrix}\omega_1^2+(\omega_2^2+\omega_3^2)\cos\theta & 2\omega_1\omega_2\sin^2\frac{1}{2}\theta-\omega_3\omega\sin\theta & 2\omega_1\omega_3\sin^2\frac{1}{2}\theta+\omega_2\omega\sin\theta\\ 2\omega_1\omega_2\sin^2\frac{1}{2}\theta+\omega_3\omega\sin\theta & \omega_2^2+(\omega_3^2+\omega_1^2)\cos\theta & 2\omega_2\omega_3\sin^2\frac{1}{2}\theta-\omega_1\omega\sin\theta\\ 2\omega_1\omega_3\sin^2\frac{1}{2}\theta-\omega_2\omega\sin\theta & 2\omega_2\omega_3\sin^2\frac{1}{2}\theta+\omega_1\omega\sin\theta & \omega_3^2+(\omega_1^2+\omega_2^2)\cos\theta\end{bmatrix}. \tag{R.24}$$

If $\gamma\neq1$ but nonzero, the answers are $\alpha=\sin\theta/(\gamma\omega)$ and $\beta=(1-\cos\theta)/(\gamma^2\omega^2)$. It follows that (R.23) and (R.24) are independent of γ, as was to be expected.

§R.7.2. Rotator from Geometry

The vector representation of the rigid motion depicted in Figure R.2 is

$$\vec{\mathbf{x}}_\theta=\vec{\mathbf{x}}\cos\theta+(\vec{\mathbf{n}}\times\vec{\mathbf{x}})\sin\theta+\vec{\mathbf{n}}(\vec{\mathbf{n}}\cdot\vec{\mathbf{x}})(1-\cos\theta)=\vec{\mathbf{x}}+(\vec{\mathbf{n}}\times\vec{\mathbf{x}})\sin\theta+\big[\vec{\mathbf{n}}\times(\vec{\mathbf{n}}\times\vec{\mathbf{x}})\big](1-\cos\theta). \tag{R.25}$$

where $\vec{\mathbf{n}}$ is $\vec{\boldsymbol{\omega}}$ normalized to unit length as per (R.10). This can be recast in matrix form by substituting $\vec{\mathbf{n}}\times\vec{\mathbf{x}}\to\mathbf{N}\mathbf{x}=\boldsymbol{\Omega}\mathbf{x}/\omega$ and $\mathbf{x}_\theta=\mathbf{R}\mathbf{x}$. On cancelling $\mathbf{x}$ we get back (R.23).

§R.8. Rotators for All Seasons

If $\boldsymbol{\omega}$ is unit-length-normalized to $\mathbf{n}$ as per (R.6), $\gamma = 1/\omega$ and $\mathbf{R} = \mathbf{I} + \sin\theta\,\mathbf{N} + (1-\cos\theta)\,\mathbf{N}^2$. This is the matrix form of (R.25). Because $\mathbf{N}^2 = \mathbf{n}\mathbf{n}^T - \mathbf{I}$, an ocassionally useful variant is

$$\mathbf{R} = \mathbf{R}^* + (1-\cos\theta)\,\mathbf{n}\,\mathbf{n}^T, \qquad \mathbf{R}^* = \cos\theta\,\mathbf{I} + \sin\theta\,\mathbf{N}. \tag{R.26}$$

In terms of the three Rodrigues-Cayley parameters b_i introduced in (R.7), $\alpha = \beta = 2\cos^2\frac{1}{2}\theta$ and $\mathbf{R} = \mathbf{I} + 2\cos^2\frac{1}{2}\theta\,(\boldsymbol{\Sigma} + \boldsymbol{\Sigma}^2)$. This can be explicitly worked out to be

$$\mathbf{R} = \frac{1}{1+b_1^2+b_2^2+b_3^2}\begin{bmatrix} 1+b_1^2-b_2^2-b_3^2 & 2(b_1b_2-b_3) & 2(b_1b_3+b_2) \\ 2(b_1b_2+b_3) & 1-b_1^2+b_2^2-b_3^2 & 2(b_2b_3-b_1) \\ 2(b_1b_3-b_2) & 2(b_2b_3+b_1) & 1-b_1^2-b_2^2+b_3^2 \end{bmatrix} \tag{R.27}$$

This form was first derived by Rodrigues [R.69] and used by Cayley [R.19, p. 332–336] to study rigid body motions. It has the advantage of being obtainable through an algebraic matrix expression: the Cayley transform, presented below. It becomes indeterminate, however, as $\theta \to 180^\circ$, since all terms approach $0/0$. This indeterminacy is avoided by using the four Euler-Rodrigues parameters, which are also the quaternion coefficients, defined in (R.8). In terms of these we get

$$\mathbf{R} = 2\begin{bmatrix} p_0^2+p_1^2-\frac{1}{2} & p_1p_2-p_0p_3 & p_1p_3+p_0p_2 \\ p_1p_2+p_0p_3 & p_0^2+p_2^2-\frac{1}{2} & p_2p_3-p_0p_1 \\ p_1p_3-p_0p_2 & p_2p_3+p_0p_1 & p_0^2+p_3^2-\frac{1}{2} \end{bmatrix} \tag{R.28}$$

This expression cannot become singular. This is paid, however, at the cost of carrying along an extra parameter in addition to the constraint $p_0^2+p_1^2+p_2^2+p_3^2 = 1$.

The normalization of Fraeijs de Veubeke [R.25] introduced in (R.9): $p_i = (\omega_i/\omega)\sin\frac{1}{2}\theta$, leads to $\alpha = 2\cos\frac{1}{2}\theta$ and $\beta = 2$. Hence $\mathbf{R} = \mathbf{I} + 2\cos\frac{1}{2}\theta\,\boldsymbol{\Omega}_p + 2\boldsymbol{\Omega}_p^2$, with $\boldsymbol{\Omega}_p = (\sin\frac{1}{2}\theta/\omega)\boldsymbol{\Omega}$.

§R.9. The Cayley Transform

Given any skew-symmetric real matrix $\boldsymbol{\Sigma} = -\boldsymbol{\Sigma}^T$, we can apply the transformation

$$\mathbf{Q} = (\mathbf{I}+\boldsymbol{\Sigma})(\mathbf{I}-\boldsymbol{\Sigma})^{-1}. \tag{R.29}$$

[Note: this mapping can be written in many different ways; some authors use $(\mathbf{I}-\boldsymbol{\Sigma})(\mathbf{I}+\boldsymbol{\Sigma})^{-1}$, some switch $\mathbf{I}$ and $\boldsymbol{\Sigma}$, while others prefer the involutory form $(\mathbf{I}+\boldsymbol{\Sigma})^{-1}(\mathbf{I}-\boldsymbol{\Sigma})$.] $\mathbf{Q}$ is a proper orthogonal matrix, that is $\mathbf{Q}^T\mathbf{Q} = \mathbf{I}$ and $\det\mathbf{Q} = +1$. This is stated in several texts, e.g., Gantmacher [R.33, p. 288] and Turnbull [R.84, p. 156] but none gives a proof for general order. Here is the orthogonality proof: $\mathbf{Q}^T\mathbf{Q} = (\mathbf{I}+\boldsymbol{\Sigma})^{-1}(\mathbf{I}-\boldsymbol{\Sigma})(\mathbf{I}+\boldsymbol{\Sigma})(\mathbf{I}-\boldsymbol{\Sigma})^{-1} = (\mathbf{I}+\boldsymbol{\Sigma})^{-1}(\mathbf{I}+\boldsymbol{\Sigma})(\mathbf{I}-\boldsymbol{\Sigma})(\mathbf{I}-\boldsymbol{\Sigma})^{-1} = \mathbf{I}^2 = \mathbf{I}$ because $\mathbf{I}+\boldsymbol{\Sigma}$ and $\mathbf{I}-\boldsymbol{\Sigma}$ commute. The property $\det\mathbf{Q} = +1$ can be shown to hold from the spectral properties of skew-symmetric matrices. The inverse transformation

$$\boldsymbol{\Sigma} = (\mathbf{Q}+\mathbf{I})^{-1}(\mathbf{Q}-\mathbf{I}), \tag{R.30}$$

produces skew-symmetric matrices from a source proper-orthogonal matrix $\mathbf{Q}$. Equations (R.29) and (R.30) are called the *Cayley transforms* after Cayley [R.20]. These formulas are sometimes useful in the construction of approximations for moderate rotations.

An interesting question is: given $\boldsymbol{\Omega}$ and θ, can (R.29) be used to produce the exact $\mathbf{R}$? The answer is: yes, if $\boldsymbol{\Omega}$ is scaled by a specific $\gamma = \gamma(\theta,\omega)$. We thus investigate whether $\mathbf{R} = (\mathbf{I}+\gamma\boldsymbol{\Omega})(\mathbf{I}-\gamma\boldsymbol{\Omega})^{-1}$ exactly for some γ. Premultiplying both sides by $\mathbf{I}-\gamma\boldsymbol{\Omega}$ and representing $\mathbf{R}$ by (R.20) we require

$$(\mathbf{I}-\gamma\boldsymbol{\Omega})(\mathbf{I}+\alpha\gamma\boldsymbol{\Omega}+\beta\gamma^2\boldsymbol{\Omega}^2) = \mathbf{I}+\gamma(\alpha-\gamma+\gamma\beta\omega^2)\boldsymbol{\Omega}+\gamma^2(\beta-\alpha)\boldsymbol{\Omega}^2 = \mathbf{I}+\gamma\boldsymbol{\Omega} \tag{R.31}$$

Identifying coefficients and assuming $\gamma \neq 0$ we get the conditions $\beta = \alpha$ and $\alpha - 1 + \beta\omega^2\gamma^2 = 1$, from which $\alpha = \beta = 2/(1+\gamma^2\omega^2)$. Equating to $\beta = 2\sin^2\frac{1}{2}\theta/(\gamma^2\omega^2)$ and solving for $\gamma\omega$ gives as only solutions $\gamma = \pm\tan\frac{1}{2}\theta/\omega$. Adopting the $+$ sign, this becomes the normalization (R.7). Consequently

$$\mathbf{R} = (\mathbf{I}+\boldsymbol{\Sigma})(\mathbf{I}-\boldsymbol{\Sigma})^{-1}, \quad \boldsymbol{\Sigma} = \frac{\tan\frac{1}{2}\theta}{\omega}\boldsymbol{\Omega}. \tag{R.32}$$

The explicit calculation of $\mathbf{R}$ in terms of the b_i leads to (R.27).

§R.10. Exponential Map

This is a final representation of $\mathbf{R}$ that has theoretical and practical importance. Given a skew-symmetric real matrix $\mathbf{W}$, the matrix exponential

$$\mathbf{Q} = e^{\mathbf{W}} = \mathbf{Exp}(\mathbf{W}) \tag{R.33}$$

is proper orthogonal. Here is the simple proof of Gantmacher [R.33, p 287]. First, $\mathbf{Q}^T = \mathbf{Exp}(\mathbf{W}^T) = \mathbf{Exp}(-\mathbf{W}^T) = \mathbf{Q}^{-1}$. Next, if the eigenvalues of $\mathbf{W}$ are λ_i, $\sum_i \lambda_i = \mathbf{trace}(\mathbf{W}) = 0$. The eigenvalues of $\mathbf{Q}$ are $\mu_i = \exp(\lambda_i)$; thus $\det(\mathbf{Q}) = \Pi_i \mu_i = \exp(\sum_i \lambda_i) = \exp(0) = +1$. The transformation (R.33) is called an *exponential map*. The converse is of course $\mathbf{W} = \mathbf{Log}_e(\mathbf{Q})$ with the principal value taken.

As in the case of the Cayley transform, one may pose the question of whether we can get the rotator $\mathbf{R} = \mathbf{Exp}(\gamma\boldsymbol{\Omega})$ exactly for some factor $\gamma = \gamma(\theta, \omega)$. To study this question we need an explicit form of the exponential. This can be obtained from the spectral form (R.14) in which the spin function is **Exp** so that the diagonal matrix entries are 1 and $\exp(\pm\gamma\omega i) = \cos\gamma\omega \pm i \sin\gamma\omega$. The following approach is more instructive and leads directly to the final result. Start from the definition of the matrix exponential

$$\mathbf{Exp}(\gamma\boldsymbol{\Omega}) = \mathbf{I} + \gamma\boldsymbol{\Omega} + \frac{\gamma^2}{2!}\boldsymbol{\Omega}^2 + \frac{\gamma^3}{3!}\boldsymbol{\Omega}^3 + \ldots \tag{R.34}$$

and use the Cayley-Hamilton theorem (R.16) to eliminate all powers of order 3 or higher in $\boldsymbol{\Omega}$. Identify the coefficient series of $\boldsymbol{\Omega}$ and $\boldsymbol{\Omega}^2$ with those of the sine and cosine, to obtain

$$\mathbf{Exp}(\gamma\boldsymbol{\Omega}) = \mathbf{I} + \frac{\sin(\gamma\omega)}{\gamma\omega}\boldsymbol{\Omega} + \frac{1-\cos(\gamma\omega)}{\gamma^2\omega^2}\boldsymbol{\Omega}^2. \tag{R.35}$$

Comparing this to (R.23) requires $\gamma\omega = \theta$, or $\gamma = \theta/\omega$. Introducing $\theta_i = \theta\omega_i/\omega$ and $\boldsymbol{\Theta} = \mathbf{Spin}(\boldsymbol{\theta}) = \theta\mathbf{N} = (\theta/\omega)\boldsymbol{\Omega}$ as in (R.10), we find

$$\mathbf{R} = \mathbf{Exp}(\boldsymbol{\Theta}) = \mathbf{I} + \frac{\sin\theta}{\theta}\boldsymbol{\Theta} + \frac{1-\cos\theta}{\theta^2}\boldsymbol{\Theta}^2 = \mathbf{I} + \frac{\sin\theta}{\theta}\boldsymbol{\Theta} + \frac{2\sin^2\frac{1}{2}\theta}{\theta^2}\boldsymbol{\Theta}^2. \tag{R.36}$$

On substituting $\boldsymbol{\Theta} = \theta\mathbf{N}$ this recovers $\mathbf{R} = \mathbf{I} + \sin\theta\,\mathbf{N} + (1-\cos\theta)\,\mathbf{N}^2$, as it should.

This representation has several advantages: it is singularity free, the parameters θ_i are exactly proportional to the angle, and the differentiation of $\mathbf{R}$ is simplified. Because of these favorable attributes the exponential map has become a favorite of implementations where very large rotations may occur, as in orbiting structures and robotics.

Remark 6. Some authors state that the exponential map is exact whereas the Cayley transform is a (1,1) Padé approximation to it. The foregoing treatment shows that the statement is incorrect. Both are exact for specific but different spinor normalizations, and inexact otherwise.

§R.11. Skew-Symmetric Matrix Relations

The following relations involving spinors are useful in some derivations. If $\mathbf{v}$ and $\mathbf{w}$ are two 3-vectors, and $\mathbf{V} = \mathbf{Spin}(\mathbf{v})$ and $\mathbf{W} = \mathbf{Spin}(\mathbf{w})$ the associated spinors, $\mathbf{VW} - \mathbf{WV}$ is skew-symmetric and

$$\mathbf{axial}(\mathbf{VW} - \mathbf{WV}) = \mathbf{Vw} = -\mathbf{Wv}. \tag{R.37}$$

Let $\mathbf{Q}$ be an arbitrary nonsingular 3×3 matrix whereas $\mathbf{W} = \mathbf{Spin}(\mathbf{w})$ is skew-symmetric. It can be easily verified that $\mathbf{Q}^T\mathbf{WQ}$ is skew-symmetric. Then

$$\det(\mathbf{Q})\,\mathbf{Q}^{-1}\mathbf{w} = \mathbf{axial}(\mathbf{Q}^T\mathbf{WQ}), \qquad \det(\mathbf{Q})\,\mathbf{Q}^{-T}\mathbf{w} = \mathbf{axial}(\mathbf{QWQ}^T). \tag{R.38}$$

If $\mathbf{Q}$ is proper orthogonal, $\mathbf{Q}^{-1} = \mathbf{Q}^T$ and $\det(\mathbf{Q}) = 1$, in which case

$$\mathbf{Q}^T\mathbf{w} = \mathbf{axial}(\mathbf{Q}^T\mathbf{WQ}), \quad \mathbf{Qw} = \mathbf{axial}(\mathbf{QWQ}^T). \tag{R.39}$$

The inverse of $\mathbf{Q} = \mathbf{I} + \alpha\mathbf{W} + \beta\mathbf{W}^2$, in which $\mathbf{W} = \mathbf{Spin}(\mathbf{w})$ is skew-symmetric, is

$$\mathbf{Q}^{-1} = \mathbf{I} + \frac{\alpha}{\alpha^2 w^2 + (\beta w^2 - 1)^2}\mathbf{W} + \frac{\alpha^2 + \beta(\beta w^2 - 1)}{\alpha^2 w^2 + (\beta w^2 - 1)^2}\mathbf{W}^2, \quad \text{with} \quad w^2 = ||\mathbf{w}||^2 = w_1^2 + w_2^2 + w_3^2. \tag{R.40}$$

§R.12. From Rotators to Spinors

If $\mathbf{R}(\mathbf{n},\theta)$ is given, the extraction of the rotation angle θ and the unit pseudo-vector $\mathbf{n}=\boldsymbol{\omega}/\omega$ is often required. The former is easy using the trace property (R.19):

$$\cos\theta = \tfrac{1}{2}\big(\mathbf{trace}(\mathbf{R})-1\big) \tag{R.41}$$

Recovery of $\mathbf{n}$ is straightforward from the unit-axial-vector form $\mathbf{R}=\mathbf{I}+\sin\theta\,\mathbf{N}+(1-\cos\theta)\mathbf{N}^2$ since $\mathbf{R}-\mathbf{R}^T = 2\sin\theta\,\mathbf{N}$, whence

$$\mathbf{N}=\frac{\mathbf{R}-\mathbf{R}^T}{2\sin\theta},\qquad \mathbf{n}=\begin{bmatrix} n_1\\ n_2\\ n_3\end{bmatrix}=\mathbf{axial}(\mathbf{N}) \tag{R.42}$$

One issue is the sign of θ since (R.41) is satisfied by $\pm\theta$. If the sign is reversed, so is $\mathbf{n}$. Thus it is possible to select $\theta\ge 0$ if no constraints are placed on the direction of the rotation axis.

The foregoing formulas are prone to numerical instability for angles near 0°, $\pm 180^\circ$, etc., because $\sin\theta$ vanishes. A robust algorithm is that given by Spurrier [R.76] in the language of quaternions. Choose the algebraically largest of $\mathbf{trace}(\mathbf{R})$ and R_{ii}, $i=1,2,3$. If $\mathbf{trace}(\mathbf{R})$ is the largest, compute

$$p_0=\cos\tfrac{1}{2}\theta=\tfrac{1}{2}\sqrt{1+\mathbf{trace}(\mathbf{R})},\qquad p_i=n_i\sin\tfrac{1}{2}\theta=\tfrac{1}{4}(R_{kj}-R_{jk})/p_0,\quad i=1,2,3, \tag{R.43}$$

where j and k are the cyclic permutations of i. Otherwise let R_{ii} be the algebraically largest diagonal entry, and again denote by i, j, k its cyclic permutation. Then use

$$\begin{aligned} &p_i=n_i\sin\tfrac{1}{2}\theta=\sqrt{\tfrac{1}{2}R_{ii}+\tfrac{1}{4}(1-\mathbf{trace}(\mathbf{R}))},\qquad p_0=\cos\tfrac{1}{2}\theta=\tfrac{1}{4}(R_{kj}-R_{jk})/p_i,\\ &p_m=\tfrac{1}{4}(R_{m,i}+R_{i,m})/p_i,\quad m=j,k. \end{aligned} \tag{R.44}$$

From p_0, p_1, p_2, p_3 it is easy to pass to θ, n_1, n_2, n_3 once the sign of θ is chosen as discussed above.

The theoretical formula for the logarithm of a 3×3 orthogonal matrix is

$$\boldsymbol{\Theta}=\mathbf{Log}_e(\mathbf{R})=\frac{\arcsin\tau}{2\tau}(\mathbf{R}-\mathbf{R}^T),\quad \boldsymbol{\Omega}=\frac{\omega}{\theta}\boldsymbol{\Theta},\quad \mathbf{N}=\frac{\boldsymbol{\Theta}}{\theta}, \tag{R.45}$$

where $\tau=\frac{1}{2}||\mathbf{axial}(\mathbf{R}-\mathbf{R}^T)||_2$. The formula fails, however, outside the range $[-\pi/2\le\theta\le\pi/2]$ and is numerically unstable near $\theta=0$.

§R.13. Spinor and Rotator Transformations

Suppose $\boldsymbol{\Omega}$ is a spinor and $\mathbf{R}=\mathbf{Rot}(\boldsymbol{\Omega})$ the associated rotator, referred to a Cartesian frame $\mathbf{x}=\{x_i\}$. It is required to transform $\mathbf{R}$ to another Cartesian frame $\bar{\mathbf{x}}=\{\bar{x}_i\}$ related by $T_{ij}=\partial\bar{x}_i/\partial x_j$, where T_{ij} are entries of a 3×3 orthogonal matrix $\mathbf{T}=\partial\bar{\mathbf{x}}/\partial\mathbf{x}$. Application of (R.18) yields

$$\bar{\mathbf{R}}=\mathbf{T}\mathbf{R}\mathbf{T}^T,\quad \bar{\mathbf{R}}^T=\mathbf{T}\mathbf{R}^T\mathbf{T}^T,\qquad \mathbf{R}=\mathbf{T}^T\bar{\mathbf{R}}\mathbf{T},\quad \mathbf{R}=\mathbf{T}^T\bar{\mathbf{R}}^T\mathbf{T}. \tag{R.46}$$

More details may be found in Chapter 4 of [R.35]. Pre and post-multiplying (R.42) by $\mathbf{T}$ and $\mathbf{T}^T$, respectively, yields the transformed spinor $\bar{\mathbf{N}}=\mathbf{T}\mathbf{N}\mathbf{T}^T$, which is also skew-symmetric because $\bar{\mathbf{N}}^T=\mathbf{T}\mathbf{N}^T\mathbf{T}^T=-\bar{\mathbf{N}}$. Likewise for the other spinors listed in Table R.5. Relations (R.39) with $\mathbf{Q}\to\mathbf{T}$ show how axial vectors transform.

§R.14. Axial Vector Jacobian

The Jacobian matrix $\mathbf{H}(\boldsymbol{\theta}) = \partial\boldsymbol{\theta}/\partial\boldsymbol{\omega}$ of the rotational axial vector $\boldsymbol{\theta}$ with respect to the spin axial vector $\boldsymbol{\omega}$, and its inverse $\mathbf{H}(\boldsymbol{\theta})^{-1} = \partial\boldsymbol{\omega}/\partial\boldsymbol{\theta}$, appear in the EICR. The latter was first derived by Simo [R.71] and Szwabowicz [R.77], and rederived by Nour-Omid and Rankin [R.54, p. 377]:

$$\mathbf{H}(\boldsymbol{\theta})^{-1} = \frac{\partial\boldsymbol{\omega}}{\partial\boldsymbol{\theta}} = \frac{\sin\theta}{\theta}\mathbf{I} + \frac{1-\cos\theta}{\theta^2}\boldsymbol{\Theta} + \frac{\theta-\sin\theta}{\theta^3}\boldsymbol{\theta}\boldsymbol{\theta}^T = \mathbf{I} + \frac{1-\cos\theta}{\theta^2}\boldsymbol{\Theta} + \frac{\theta-\sin\theta}{\theta^3}\boldsymbol{\Theta}^2. \tag{R.47}$$

The last expression in (R.47), not given by the cited authors, is obtained on replacing $\boldsymbol{\theta}\boldsymbol{\theta}^T = \theta^2\mathbf{I} + \boldsymbol{\Theta}^2$. Use of the inversion formula (R.40) gives

$$\mathbf{H}(\boldsymbol{\theta}) = \frac{\partial\boldsymbol{\theta}}{\partial\boldsymbol{\omega}} = \mathbf{I} - \tfrac{1}{2}\boldsymbol{\Theta} + \eta\boldsymbol{\Theta}^2 \quad \text{with} \quad \eta = \frac{1-\frac{1}{2}\theta\cot(\frac{1}{2}\theta)}{\theta^2} = \tfrac{1}{12} + \tfrac{1}{720}\theta^2 + \tfrac{1}{30240}\theta^4 + \tfrac{1}{1209600}\theta^6 + \ldots \tag{R.48}$$

The η given in (R.48) results by simplifying the value $\eta = [\sin\theta - \theta(1+\cos\theta)]/[\theta^2\sin\theta]$ given by previous investigators. Care must be taken on evaluating η for small angle θ because it approaches $0/0$; if $|\theta| < 1/20$, say, the series given above may be used, with error $< 10^{-16}$ when 4 terms are retained. If θ is a multiple of 2π, η blows up since $\cot(\frac{1}{2}\theta) \to \infty$, and a modulo-$2\pi$ reduction is required.

In the formulation of the tangent stiffness matrix the spin derivative of $\mathbf{H}(\boldsymbol{\theta})^T$ contracted with a nodal moment vector $\mathbf{m}$ is required:

$$\mathbf{L}(\boldsymbol{\theta},\mathbf{m}) = \frac{\partial\mathbf{H}(\boldsymbol{\theta})^T}{\partial\boldsymbol{\omega}}:\mathbf{m} = \frac{\partial}{\partial\boldsymbol{\theta}}[\mathbf{H}(\boldsymbol{\theta})^T\mathbf{m}]\,\mathbf{H}(\boldsymbol{\theta}) = \left\{\eta\,[(\boldsymbol{\theta}^T\mathbf{m})\,\mathbf{I} + \boldsymbol{\theta}\,\mathbf{m}^T - 2\mathbf{m}\,\boldsymbol{\theta}^T] + \mu\boldsymbol{\Theta}^2\,\mathbf{m}\,\boldsymbol{\theta}^T - \tfrac{1}{2}\mathbf{Spin}(\mathbf{m})\right\}\mathbf{H}(\boldsymbol{\theta}). \tag{R.49}$$

in which

$$\mu = \frac{d\eta/d\theta}{\theta} = \frac{\theta^2 + 4\cos\theta + \theta\sin\theta - 4}{4\theta^4\sin^2(\frac{1}{2}\theta)} = \tfrac{1}{360} + \tfrac{1}{7560}\theta^2 + \tfrac{1}{201600}\theta^4 + \tfrac{1}{5987520}\theta^6 + \ldots \tag{R.50}$$

This expression of μ was obtained by simplifying results given in [R.54, p. 378].

§R.15. Spinor and Rotator Differentiation

Derivatives, differentials and variations of axial vectors, spinors and rotators with respect to various choices of independent variables appear in applications of finite rotations to mechanics. In this section we present only expressions that are useful in the CR description. They are initially derived for dynamics and then specialized to variations. Several of the formulas are new.

§R.15.1. Angular Velocities

We assume that the rotation angle $\boldsymbol{\theta}(t) = \theta(t)\mathbf{n}(t)$ is a given function of time t, which is taken as the independent variable. The time derivative of $\boldsymbol{\Theta}(t)$ is $\dot{\boldsymbol{\Theta}} = \mathbf{axial}(\dot{\boldsymbol{\theta}})$. To express rotator differentials in a symmetric manner we introduce an axial vector $\dot{\boldsymbol{\phi}}$ and a spinor $\dot{\boldsymbol{\Phi}} = \mathbf{Spin}(\dot{\boldsymbol{\phi}})$, related to $\dot{\boldsymbol{\Theta}}$ congruentially through the rotator:

$$\dot{\boldsymbol{\Theta}} = \mathbf{Spin}(\dot{\boldsymbol{\theta}}) = \begin{bmatrix} 0 & -\dot\theta_3 & \dot\theta_2 \\ \dot\theta_3 & 0 & -\dot\theta_1 \\ -\dot\theta_2 & \dot\theta_1 & 0 \end{bmatrix} = \mathbf{R}\dot{\boldsymbol{\Phi}}\mathbf{R}^T, \quad \dot{\boldsymbol{\Phi}} = \mathbf{Spin}(\dot{\boldsymbol{\phi}}) = \begin{bmatrix} 0 & -\dot\phi_3 & \dot\phi_2 \\ \dot\phi_3 & 0 & -\dot\phi_1 \\ -\dot\phi_2 & \dot\phi_1 & 0 \end{bmatrix} = \mathbf{R}^T\dot{\boldsymbol{\Theta}}\mathbf{R}. \tag{R.51}$$

From (R.39) it follows that the axial vectors are linked by

$$\dot{\boldsymbol{\phi}} = \mathbf{R}^T\dot{\boldsymbol{\theta}}, \qquad \dot{\boldsymbol{\theta}} = \mathbf{R}\dot{\boldsymbol{\phi}}. \tag{R.52}$$

Corresponding relation between variations or differentials, such as $\delta\boldsymbol{\Theta} = \mathbf{R}\,\delta\boldsymbol{\Phi}\,\mathbf{R}^T$ or $d\boldsymbol{\Theta} = \mathbf{R}\,d\boldsymbol{\Phi}\,\mathbf{R}^T$ are incorrect as shown in below. In CR dynamics, $\dot{\boldsymbol{\theta}}$ is the vector of *inertial angular velocities* whereas $\dot{\boldsymbol{\phi}}$ is the vector of *dynamic angular velocities*.

Repeated temporal differentiation of $\mathbf{R} = \mathbf{Exp}(\mathbf{\Theta})$ gives the rotator time derivatives

$$\dot{\mathbf{R}} = \dot{\mathbf{\Theta}}\,\mathbf{R}, \quad \ddot{\mathbf{R}} = (\ddot{\mathbf{\Theta}} + \dot{\mathbf{\Theta}}^2)\mathbf{R}, \quad \dddot{\mathbf{R}} = (\dddot{\mathbf{\Theta}} + 2\ddot{\mathbf{\Theta}}\dot{\mathbf{\Theta}} + \dot{\mathbf{\Theta}}\ddot{\mathbf{\Theta}} + \dot{\mathbf{\Theta}}^3)\mathbf{R}, \ \ldots \tag{R.53}$$

$$\dot{\mathbf{R}} = \mathbf{R}\,\dot{\mathbf{\Phi}}, \quad \ddot{\mathbf{R}} = \mathbf{R}(\ddot{\mathbf{\Phi}} + \dot{\mathbf{\Phi}}^2), \quad \dddot{\mathbf{R}} = \mathbf{R}(\dddot{\mathbf{\Phi}} + 2\ddot{\mathbf{\Phi}}\dot{\mathbf{\Phi}} + \dot{\mathbf{\Phi}}\ddot{\mathbf{\Phi}} + \dot{\mathbf{\Phi}}^3), \ \ldots \tag{R.54}$$

The following four groupings appear often: $\mathbf{R}\,\dot{\mathbf{R}}^T$, $\dot{\mathbf{R}}\,\mathbf{R}^T$, $\mathbf{R}^T\,\dot{\mathbf{R}}$ and $\dot{\mathbf{R}}^T\,\mathbf{R}$. From the identities $\mathbf{R}\mathbf{R}^T = \mathbf{I}$ and $\mathbf{R}^T\mathbf{R} = \mathbf{I}$ it can be shown that they are skew-symmetric, and may be associated to axial vectors with physical meaning. For example, taking time derivatives of $\mathbf{R}\mathbf{R}^T = \mathbf{I}$ yields $\mathbf{R}\,\dot{\mathbf{R}}^T + \dot{\mathbf{R}}\,\mathbf{R}^T = \mathbf{0}$, whence $\mathbf{R}\,\dot{\mathbf{R}}^T = -\dot{\mathbf{R}}\,\mathbf{R}^T = -(\mathbf{R}\,\dot{\mathbf{R}})^T$. Pre and postmultiplication of $\dot{\mathbf{R}}$ in (R.53) and (R.54) by $\mathbf{R}$ and $\mathbf{R}^T$ furnishes

$$\dot{\mathbf{R}}\,\mathbf{R}^T = -\mathbf{R}\,\dot{\mathbf{R}}^T = \dot{\mathbf{\Theta}}, \qquad \mathbf{R}^T\,\dot{\mathbf{R}} = -\dot{\mathbf{R}}^T\mathbf{R} = \dot{\mathbf{\Phi}}. \tag{R.55}$$

Note that the general integral of $\dot{\mathbf{R}} = \dot{\mathbf{\Theta}}\,\mathbf{R}$ aside from a constant, is $\mathbf{R} = \mathbf{Exp}(\mathbf{\Theta})$, from which $\theta(t)$ can be extracted. On the other hand there is no integral relation defining $\phi(t)$; only the differential equation $\dot{\mathbf{R}} = \mathbf{R}\,\dot{\mathbf{\Phi}}$.

§R.15.2. Angular Accelerations

Postmultiplying the second of (R.53) by $\mathbf{R}^T$ yields

$$\ddot{\mathbf{R}}\mathbf{R}^T = \ddot{\mathbf{\Theta}} + \dot{\mathbf{\Theta}}^2 = \dot{\mathbf{\Theta}} + \dot{\boldsymbol{\theta}}\,\dot{\boldsymbol{\theta}}^T - (\dot{\theta})^2\mathbf{I} = \begin{bmatrix} 0 & -\ddot{\theta}_3 & \ddot{\theta}_2 \\ \ddot{\theta}_3 & 0 & -\ddot{\theta}_1 \\ -\ddot{\theta}_2 & \ddot{\theta}_1 & 0 \end{bmatrix} + \begin{bmatrix} -\dot{\theta}_2^2 - \dot{\theta}_3^2 & \dot{\theta}_1\dot{\theta}_2 & \dot{\theta}_1\dot{\theta}_3 \\ \dot{\theta}_1\dot{\theta}_2 & -\dot{\theta}_3^2 - \dot{\theta}_1^2 & \dot{\theta}_2\dot{\theta}_3 \\ \dot{\theta}_1\dot{\theta}_3 & \dot{\theta}_2\dot{\theta}_3 & -\dot{\theta}_1^2 - \dot{\theta}_2^2 \end{bmatrix}, \tag{R.56}$$

in which $(\dot{\theta})^2 = \dot{\theta}_1^2 + \dot{\theta}_2^2 + \dot{\theta}_3^2$. When applied to a vector $\mathbf{r}$, $(\ddot{\mathbf{\Theta}} + \dot{\mathbf{\Theta}}\dot{\mathbf{\Theta}})\mathbf{r} = \ddot{\boldsymbol{\theta}} \times \mathbf{r} + \dot{\boldsymbol{\theta}}\,\dot{\boldsymbol{\theta}}^T\mathbf{r} - (\dot{\theta})^2\mathbf{r}$. This operator appears in the expression of particle accelerations in a moving frame. The second and third term give rise to the Coriolis and centrifugal forces, respectively. Premultiplying the second derivative in (R.54) by $\mathbf{R}$ yields $\mathbf{R}\ddot{\mathbf{R}} = \ddot{\mathbf{\Phi}} + \dot{\mathbf{\Phi}}\dot{\mathbf{\Phi}}$, and so on.

§R.15.3. Variations

Some of the foregoing expressions can be directly transformed to variational and differential forms while others cannot. For example, varying $\mathbf{R} = \mathbf{Exp}(\mathbf{\Theta})$ gives

$$\delta\mathbf{R} = \delta\mathbf{\Theta}\,\mathbf{R}, \qquad \delta\mathbf{R}^T = -\mathbf{R}^T\,\delta\mathbf{\Theta}. \tag{R.57}$$

This matches $\dot{\mathbf{R}} = \dot{\mathbf{\Theta}}\,\mathbf{R}$ and $\mathbf{R}^T = -\mathbf{R}^T\dot{\mathbf{\Theta}}$ from (R.53) on replacing $\dot{(\,)}$ by δ. On the other hand, the counterparts of (R.54): $\dot{\mathbf{R}} = \mathbf{R}\,\dot{\mathbf{\Phi}}$ and $\dot{\mathbf{R}}^T = -\dot{\mathbf{\Phi}}\,\mathbf{R}$ are *not* $\delta\mathbf{R} = \mathbf{R}\,\delta\mathbf{\Phi}$ and $\delta\mathbf{R}^T = -\delta\mathbf{\Phi}\,\mathbf{R}^T$, a point that has tripped authors unfamiliar with moving frame dynamics. Correct handling requires the introduction of a third axial vector $\boldsymbol{\psi}$:

$$\delta\mathbf{R} = \mathbf{R}\,\delta\mathbf{\Psi}, \quad \delta\mathbf{R}^T = -\delta\mathbf{\Psi}\,\mathbf{R}, \quad \text{in which} \quad \delta\mathbf{\Psi} = \mathbf{Spin}(\delta\boldsymbol{\psi}) = \begin{bmatrix} 0 & -\delta\psi_3 & \delta\psi_2 \\ \delta\psi_3 & 0 & -\delta\psi_1 \\ -\delta\psi_2 & \delta\psi_1 & 0 \end{bmatrix} \tag{R.58}$$

Axial vectors $\boldsymbol{\psi}$ and $\boldsymbol{\phi}$ can be linked as follows. Start from $\delta\mathbf{R} = \mathbf{R}\,\delta\mathbf{\Psi}$ and $\dot{\mathbf{R}} = \mathbf{R}\,\dot{\mathbf{\Phi}}$. Time differentiate the former: $\delta\dot{\mathbf{R}} = \mathbf{R}\,\delta\dot{\mathbf{\Psi}} + \dot{\mathbf{R}}\,\delta\mathbf{\Psi}$, and vary the latter: $\delta\dot{\mathbf{R}} = \delta\mathbf{R}\,\dot{\mathbf{\Phi}} + \mathbf{R}\,\delta\dot{\mathbf{\Phi}}$, equate the two right-hand sides, premultiply by $\mathbf{R}^T$, replace $\mathbf{R}^T\dot{\mathbf{R}}$ and $\mathbf{R}^T\delta\mathbf{R}$ by $\dot{\mathbf{\Phi}}$ and $\delta\mathbf{\Psi}$, respectively, and rearrange to obtain

$$\delta\dot{\mathbf{\Phi}} = \delta\dot{\mathbf{\Psi}} + \dot{\mathbf{\Phi}}\,\delta\mathbf{\Psi} - \delta\mathbf{\Psi}\,\dot{\mathbf{\Phi}}, \quad \text{or} \quad \delta\dot{\boldsymbol{\phi}} = \delta\dot{\boldsymbol{\psi}} + \dot{\mathbf{\Phi}}\,\delta\boldsymbol{\psi} = \delta\dot{\boldsymbol{\psi}} - \delta\mathbf{\Psi}\,\dot{\boldsymbol{\phi}}. \tag{R.59}$$

The last transformation is obtained by taking the axial vectors of both sides, and using (R.37). It is seen that $\delta\dot{\mathbf{\Psi}}$ and $\delta\dot{\mathbf{\Phi}}$ match if and only if $\dot{\mathbf{\Phi}}$ and $\delta\mathbf{\Psi}$ commute.

Higher variations and differentials can be obtained through similar techniques. The general rule is: if there is a rotator integral such as $\mathbf{R} = \mathbf{Exp}(\mathbf{\Theta})$, time derivatives can be directly converted to variations. If no integral exists, utmost care must be exerted. Physically quantities such as $\boldsymbol{\phi}$ and $\boldsymbol{\psi}$ are related to a moving frame, which makes differential relations rheonomic.

§R.16. CR Matrices for Triangular Shell Element

The element types tested in Part II [R.38] are shown in Figure R.3. Each element has 6 degrees of freedom (DOF) per node: three translations and three rotations. Shells include the drilling DOF. The linear internal force and stiffness matrix of the shell elements are constructed with the Assumed Natural Deviatoric Strain (ANDES) formulation [R.27–R.32,R.53] in terms of the deformational displacements and rotations. ANDES is a direct descendent of the Assumed Natural Strain (ANS) formulation of Park and Stanley [R.59] and the Free Formulation of Bergan and coworkers [R.11–R.14]. The derivation of the linear models is outlined in Part II [R.38].

The matrices required to implement the EICR are **T**, **P**, **S**, **G**, **H** and **L**. None of these depend on how the internal element force $\bar{\mathbf{p}}^e$ and stiffness matrix $\bar{\mathbf{K}}^e$ of the small-strain linear element are formed. In terms of implementation the EICR matrices can be classified into two groups:

(i) **T**, **H** and **L**, as well as the T-projector component $\mathbf{P}_u$ of **P**, are block diagonal matrices built up with 3×3 node blocks. These blocks can be formed by standard modules which are *independent of the element type*, as long as the element has the standard 6 DOFs per node. The only difference is the number of nodes.

(ii) The R-projector component of **P**, which is $\mathbf{P}_\omega = \mathbf{SG}$, does depend on element type, geometry and choice of CR frame through matrix **G**. These must be recoded for evry change in those attributes.

In this Appendix we give the **G** and **S** matrices that appear in the "front end" of the EICR for the triangular shell element, as that illustrates the effect of CR frame selection. Matrices for the beam and quadrilateral element are given in Part II.

In the following sections, element axes labels are changed from $\{\bar{x}_1, \bar{x}_2, \bar{x}_3\}$ to $\{\bar{x}, \bar{y}, \bar{z}\}$ to unclutter nodal subscripting. Likewise the displacement components $\{\bar{u}_1, \bar{u}_2, \bar{u}_3\}$ are relabeled $\{\bar{u}_x, \bar{u}_y, \bar{u}_z\}$.

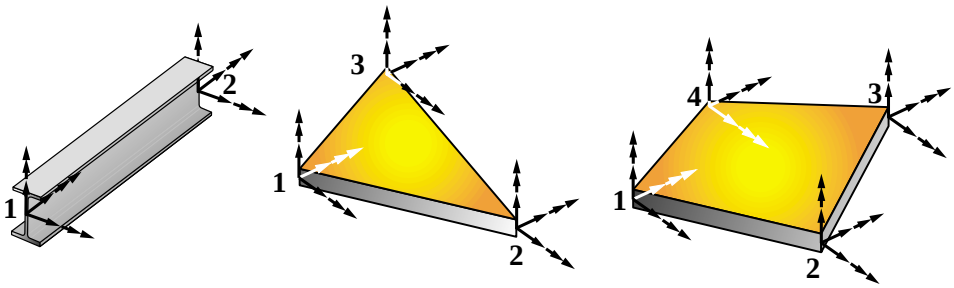

FIGURE R.3. Elements tested in Part II.

§R.17. Matrix $\bar{\mathbf{S}}$

This 18×3 lever matrix is given by (written in transposed form to save space)

$$\bar{\mathbf{S}} = [\, -\mathbf{Spin}(\bar{\mathbf{x}}_1) \quad \mathbf{I} \quad -\mathbf{Spin}(\bar{\mathbf{x}}_2) \quad \mathbf{I} \quad -\mathbf{Spin}(\bar{\mathbf{x}}_3) \quad \mathbf{I}\,]^T \tag{R.60}$$

where **I** is the 3×3 identity matrix, and $\bar{\mathbf{x}}_a = [\, \bar{x}_a, \bar{y}_a, \bar{z}_a\,]^T$, the position vector of node a in the deformed (current) configuration, measured in the element CR frame.

§R.18. Matrix $\bar{\mathbf{G}}$

This 3×18 matrix connects the variation in rigid element spin to the incremental translations and spins at the nodes, both with respect to the CR frame. **G** decomposes into three 3×6 submatrices, one for each node:

$$\delta\boldsymbol{\omega}_r = \bar{\mathbf{G}}\,\delta\bar{\mathbf{v}}, \quad \mathbf{G} = [\,\mathbf{G}_1 \;\; \mathbf{G}_2 \;\; \mathbf{G}_3\,], \quad \delta\bar{\mathbf{v}} = \begin{bmatrix} \delta\bar{\mathbf{v}}_1 \\ \delta\bar{\mathbf{v}}_2 \\ \delta\bar{\mathbf{v}}_3 \end{bmatrix}, \quad \delta\bar{\mathbf{v}}_a = \begin{bmatrix} \delta\bar{\mathbf{u}}_a \\ \delta\bar{\boldsymbol{\omega}}_a \end{bmatrix}, \quad a = 1, 2, 3. \tag{R.61}$$

Submatrices $\mathbf{G}_a$ depend on how the element CR frame is chosen. The origin of the frame is always placed at the element centroid. But various methods have been used to direct the axes $\{\bar{x}_i\}$. Three methods used in the present research are described.

§R.18.1. $\bar{\mathbf{G}}$ by Side Alignment

This procedure is similar to that used by Rankin and coworkers [R.54,R.63–R.66]. They select side 1–3 for $\bar{x}_2$ and node 1 as frame origin. The approach used here aligns $\bar{x}_1$ with side 1–2 and picks the centroid as origin. Then

$$\bar{\mathbf{G}}_1 = \frac{1}{2A}\begin{bmatrix} 0 & 0 & \bar{x}_{32} & 0 & 0 & 0 \\ 0 & 0 & \bar{y}_{32} & 0 & 0 & 0 \\ 0 & -h_3 & 0 & 0 & 0 & 0 \end{bmatrix}, \quad \bar{\mathbf{G}}_2 = \frac{1}{2A}\begin{bmatrix} 0 & 0 & \bar{x}_{13} & 0 & 0 & 0 \\ 0 & 0 & \bar{y}_{13} & 0 & 0 & 0 \\ 0 & h_3 & 0 & 0 & 0 & 0 \end{bmatrix}, \quad \bar{\mathbf{G}}_3 = \frac{1}{2A}\begin{bmatrix} 0 & 0 & \bar{x}_{32} & 0 & 0 & 0 \\ 0 & 0 & \bar{y}_{32} & 0 & 0 & 0 \\ 0 & 0 & 0 & 0 & 0 & 0 \end{bmatrix}, \tag{R.62}$$

where $h_3 = 2A/L_3$ is the distance of corner 3 to the opposite side, A the triangle area, and L_3 the length of side 12. This choice satisfies the decomposition property (13.10) that guards against unbalanced force effects while iterating for equilibrium. On the other hand it violates invariance: the choice of CR frame depends on node numbering, and different results may be obtained if the mesh is renumbered.

§R.18.2. G by Least Square Angular Fit

Nygård [R.57] and Bjærum [R.18] place $\mathcal{C}^R$ in the plane of the deformed element with origin at node 1. The inplane orientation of the CR element is determined by a least square fit of the side angular errors. Referring to Figure R.4 the squared error is $d^2 = \phi_1^2 + \phi_2^2 + \phi^2$. Rotating by an additional angle χ this becomes $d^2(\chi) = (\phi_1+\chi)^2+(\phi_2+\chi)^2+(\phi+\chi)^2$. Miniminization respect to χ: $\partial d^2/\partial\chi = 0$ yields $\chi = -(\phi_1+\phi_2+\phi_3)/3$. Consequently the optimal in-plane position according to this criterion is given by the mean of the side angular errors.

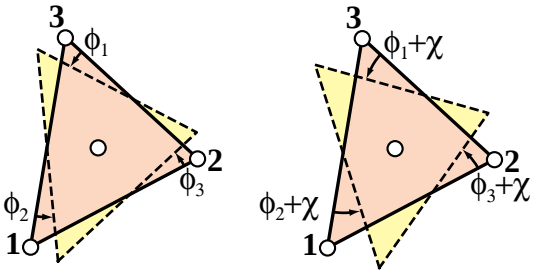

FIGURE R.4. Side angular error measure for triangular shell element.

This condition yields for the nodal submatrices

$$\bar{\mathbf{G}}_i = \frac{1}{2A}\begin{bmatrix} 0 & 0 & \bar{x}_{kj} & 0 & 0 & 0 \\ 0 & 0 & \bar{y}_{kj} & 0 & 0 & 0 \\ \frac{2A}{3}(-\frac{s_{jy}}{l_j}+\frac{s_{ky}}{L_k}) & \frac{2A}{3}(\frac{s_{jx}}{l_j}-\frac{s_{kx}}{L_k}) & 0 & 0 & 0 & 0 \end{bmatrix}. \tag{R.63}$$

where L_i is the side length opposite corner i and $\{s_{kx}, s_{ky}\}$ the projections of that side on the $\{x, y\}$ axes. An advantage of this fitting method is that it satisfies invariance with respect to node numbering. On the other hand, the rotator gradient matrix cannot be decomposed as in (13.10) leading to an approximate projector away from equilibrium. This disadvantage is not serious for a flat triangular element, however, since the CR and deformed configurations remain close on the assumption of small membrane strains.

A more serious shortcoming is that the procedure reintroduces the problem of spurious normal-to-the-plane rotations when an element with drilling freedoms is subjected to pure stretch. The difficulty is illustrated in Figure R.5, where a two triangle patch is subject to uniform stretch in the $\bar{y}$ direction. Under this state all rotations should vanish. The elements do rotate, however, because of the in-plane skewing of the diagonal. A deformational rotation is picked up since a predictor step gives no drilling rotations at the nodes, whereas the deformational drilling rotation is the total minus the rigid body rotation: $\theta_d = \theta - \theta_r$.

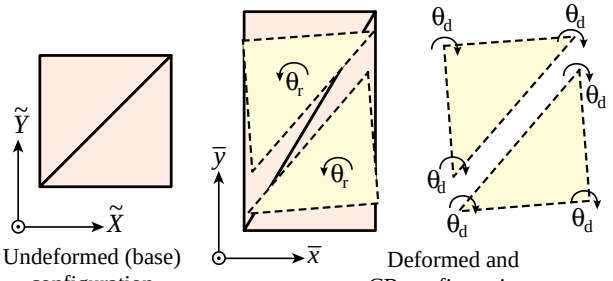

FIGURE R.5. Finite stretch patch test for two triangle elements equipped with corner drilling freedoms.

The problem is analogous to that discussed by Irons and Ahmad [R.45, p. 289] when defining node drilling freedoms as the mean of rotations of element sides meeting at that node; such elements grossly violate the patch test. This difficulty was overcome by Bergan and Felippa [R.14] by defining the node drilling freedom as the continuum mechanics rotation $\theta_z = \frac{1}{2}(\partial\bar{u}_y/\partial\bar{x} - \partial\bar{u}_x/\partial\bar{y})$ at the node. It is seen that the problem of spurious drilling rotations has been reintroduced for the nonlinear case by the choice of CR frame positioning. In fact this problem becomes even more serious with the side alignment procedure described in the foregoing subsection.

§R.18.3. Fit According to CST Rotation

The infinitesimal drilling rotation of a plane stress CST element (Turner triangle, linear triangle), is given by [R.27,R.32]

$$\bar{\theta}^{lin}_{CST} = \tfrac{1}{2}\left(\frac{\partial \bar{u}_y}{\partial \bar{x}} - \frac{\partial \bar{u}_x}{\partial \bar{y}}\right) = \frac{1}{4A}\left(\bar{x}_{23}\bar{u}_{x1} + \bar{x}_{31}\bar{u}_{x2} + \bar{x}_{12}\bar{u}_{x3} + \bar{y}_{23}u_{y1} + \bar{y}_{31}\bar{u}_{y2} + \bar{y}_{12}\bar{u}_{y3}\right). \tag{R.64}$$

in which $\bar{x}_{ij} = \bar{x}_i - \bar{x}_j$, $\bar{y}_{ij} = \bar{x}_i - \bar{y}_j$, etc. The extension of this result to finite rotations can be achieved through a mean finite strain rotation introduced by Novozhilov [R.55, p. 31]; cf. also [R.81, Sec. 36]:

$$\tan\bar{\theta}_{CST} = \frac{\bar{\theta}^{lin}_{CST}}{\sqrt{(1+\bar{\epsilon}_{xx})(1+\bar{\epsilon}_{yy}) - \frac{1}{4}\bar{\gamma}^2_{xy}}} \tag{R.65}$$

in which $\epsilon_{xx} = \partial\bar{u}_x/\partial\bar{x}$, $\bar{\epsilon}_{yy} = \partial\bar{u}_y/\partial\bar{y}$ and $\bar{\gamma}_{xy} = \partial\bar{u}_y/\partial\bar{x} + \partial\bar{u}_x/\partial\bar{y}$ are the infinitesimal strains (constant over the triangle) computed from the CST displacements. Novozhilov proves that this rotation measure is invariant with respect to the choice of CR axes $\{\bar{x}, \bar{y}\}$ since it is obtained as a rotational mean taken over a 2π sweep about $\bar{z}$. If this result is applied to the finite stretch path test of Figure R.5 it is found that the CR frames of both elements do not rotate, and the test is passed. The rotation gradient submatrices are

$$\tilde{\mathbf{G}}_i = \frac{1}{2A}\begin{bmatrix} 0 & 0 & \bar{x}_{kj} & 0 & 0 & 0 \\ 0 & 0 & \bar{y}_{kj} & 0 & 0 & 0 \\ -\frac{1}{2}\bar{x}_{kj} & -\frac{1}{2}\bar{y}_{kj} & 0 & 0 & 0 & 0 \end{bmatrix} \tag{R.66}$$

where j, k denote cyclic permutations of $i = 1, 2, 3$. The resulting **G** matrix satisfies the geometric separabilty condition.

§R.18.4. Best Fit by Minimum LS Deformation

The best fit solution by least-squares minimization of relative displacements given in Appendix C as equation (R.74) was obtained in 2000 [R.29]. Unlike the previous ones it has not been tested as part of a CR shell program. The measure is invariant, but it is not presently known whether it passes the stretch patch test, or if the associated **G** satisfies the geometric separability condition (13.10).

§R.19. Best Fit CR Frame

To define the CR frame of an individual element e we must find **c** and $\mathbf{R}_0$ from the following information. (In what follows the element index e is suppressed for brevity.)

(i) The geometry of the base element. This is defined through **x**, which is kept fixed.

(ii) The motion, as defined by the total displacement field **v**(**x**) recorded in the global frame as stated in Table R.2.

In dynamic analysis there is a third source of data:

(iii) Mass distribution. Associated with each **x** in $\mathcal{C}^0$ there is a volume element dV and a mass density ρ giving a mass element $dm = \rho\, dV$. This mass may include nonstructural components. The case of time-varying mass because of fuel consumption or store drop is not excluded.

Finding **c** and $\mathbf{R}_0$ as functions of **x** and **v**, plus the mass distribution in case of dynamics, is the *shadowing problem* introduced previously. What criterion should be used to determine **c** and $\mathbf{R}_0$? Clearly some nonnegative functional of the motion (but not the motion history) should be minimized. Desirable properties of the functional are:

Versatility. It must work for statics, dynamics, rigid bodies and nonstructural bodies (e.g., a fuel tank). These requirements immediately rule out any criterion that involves the strain energy, because it cannot be used for a nonstructural or rigid body.

Invariance. Should be insensitive to element node numbering. It would be disconcerting for a user to get different answers depending on how mesh nodes are numbered.

Rigid Bodies. For a rigid body, it should give the same results as a body-attached frame. This simplifies the coupling of FEM-CR and multibody dynamics codes.

Finite Stretch Patch Test Satisfaction. If a group of elements is subjected to a uniform stretch, no spurious deformational rotations should appear. This test is particularly useful when considering shell elements with drilling freedoms, as discussed in Section B.2 for the triangle.

Fraeijs de Veubeke [R.25] proposed two criteria applicable to flexible and rigid bodies: minimum kinetic energy of relative motion, and minimum Euclidean norm of the deformational displacement field. As both lead to similar results for dynamics and the first one is not applicable to statics, the second criterion is used here.

An open research question is whether a universal best fit criterion based on the polar decomposition of the element motion could be developed.

§R.20. Minimization Conditions

In statics the density ρ may be set to unity and mass integrals become volume integrals. These are taken over the base configuration, whence $\int \ldots dV$ means $\int_{\mathcal{C}^0} \ldots dV$. Furthermore the element global frame is made to coincide with the base frame to simplify notation. Thus $\mathbf{x} \equiv \tilde{\mathbf{x}}$, $\mathbf{u} \equiv \tilde{\mathbf{u}}$ and $\mathbf{a} = \mathbf{0}$. Coordinates $\mathbf{x}^0$ and $\mathbf{x}^R$ of the base are relabeled $\mathbf{X}$ and $\mathbf{x} = \mathbf{X} + \mathbf{u}$, respectively, to avoid supercripts clashing with transpose signs. Because C^0 is by definition at the base element centroid

$$\int \mathbf{X}\, dV = 0. \tag{R.67}$$

The centroid C of $\mathcal{C}^D$ is located by the condition $\int \mathbf{x}\, dV = \int (\mathbf{X} + \mathbf{u})\, dV = \int \mathbf{u}\, dV = \mathbf{c}\, V$, where $V = \int dV$ is the element volume. From (12.22) with $\mathbf{a} = \mathbf{0}$ and $\mathbf{x}^0 \to \mathbf{X}$, the best-fit functional is

$$J[\mathbf{c}, \mathbf{R}_0] = \tfrac{1}{2} \int \mathbf{u}_d^T \mathbf{u}_d \; dV = \tfrac{1}{2} \int \big[\mathbf{u} - \mathbf{c} + (\mathbf{I} - \mathbf{R}_0)\, \mathbf{X}\big]^T \big[\mathbf{u} - \mathbf{c} + (\mathbf{I} - \mathbf{R}_0)\, \mathbf{X}\big]\, dV \tag{R.68}$$

Minimizing $\bar{\mathbf{u}}_d^T \bar{\mathbf{u}}_d$ leads to the same result, since $\mathbf{u}_d$ and $\bar{\mathbf{u}}_d$ only differ by a rotator.

§R.21. Best Origin

Denote by $\Delta\mathbf{c}$ the distance between C_R and C. Taking the variation of J with respect to $\mathbf{c}$ yields

$$\begin{aligned} \frac{\partial J}{\partial \mathbf{c}}\, \delta\mathbf{c} &= -\int (\delta\mathbf{c})^T\, \mathbf{u}_d \; dV = -\,\delta\mathbf{c}^T \int \big[\mathbf{u} - \mathbf{c} + (\mathbf{I} - \mathbf{R}_0)\, \mathbf{X}\big]\, dV = -\,\delta\mathbf{c}^T \int (\mathbf{u} - \mathbf{c})\, dV = 0, \\ \Rightarrow \quad \mathbf{c} \int dV &= \mathbf{c}V = \int \mathbf{u}\, dV = (\mathbf{c} + \Delta\mathbf{c})\, V. \end{aligned} \tag{R.69}$$

where (R.67) has been used. Consequently $\Delta\mathbf{c} = \mathbf{0}$. That is, the centroids of $\mathcal{C}^R$ and $\mathcal{C}$ must coincide: $C_R \equiv C$.

§R.22. Best Rotator

The variation with respect to $\mathbf{R}_0$ gives the condition

$$\frac{\partial J}{\partial \mathbf{R}_0}\, \delta\mathbf{R}_0 = \int \mathbf{X}^T\, \delta\mathbf{R}_0 \big[\mathbf{u} - \mathbf{c} + (\mathbf{I} - \mathbf{R}_0)\, \mathbf{X}\big]\, dV = 0. \tag{R.70}$$

Replacing $\delta\mathbf{R}_0 = \delta\boldsymbol{\Theta}\, \mathbf{R}_0$ and noting that $\mathbf{X}^T\, \delta\boldsymbol{\Theta}\, \mathbf{X} = 0$ and $\int \mathbf{X}^T\, \delta\boldsymbol{\Theta}\, \mathbf{R}_0\, \mathbf{c}\, dV = 0$ yields

$$\int \mathbf{X}^T\, \delta\boldsymbol{\Theta}\, \mathbf{R}_0 \big(\mathbf{X} + \mathbf{u}\big)\, dV = \int \mathbf{X}^T \big(\delta\boldsymbol{\theta} \times \mathbf{R}(\mathbf{X} + \mathbf{u})\big)\, dV = 0. \tag{R.71}$$

Applying (R.71) to each angular variation: $\delta\theta_1$, $\delta\theta_2$ and $\delta\theta_3$ of $\delta\boldsymbol{\Theta}$ in turn, provides three nonlinear scalar equations to determine the three parameters that define $\mathbf{R}_0$. For the two-dimensional case, in which only $\delta\theta_3$ is varied and $\mathbf{R}_0$ depends only on $\theta = \theta_3$, the following equation is obtained:

$$\int \Big[(X_1 + u_1)(x_2 \cos\theta_3 - X_1 \sin\theta_3) - (X_2 + u_2)(x_1 \cos\theta_3 + X_2 \sin\theta_3)\Big]\, dV = 0, \tag{R.72}$$

whence

$$\tan\theta_3 = \frac{\int (X_2 u_1 - X_1 u_2)\, dV}{\int \Big[X_1(X_1 + u_1) + X_2(X_2 + u_2)\Big]\, dV} = \frac{\int (X_2 u_1 - X_1 u_2)\, dV}{\int (X_1 x_1 + Y_2 x_2)\, dV}. \tag{R.73}$$

For the three-dimensional case a closed form solution is not available. This is an open research topic. Fraeijs de Veubeke [R.25] reduces (R.71) to an eigenvalue problem in the axial vector of $\mathbf{R}_0$, with a subsidiary condition handled by a Lagrange multiplier. Rankin [R.67] derives a system equivalent to (R.71) for an individual finite element by lumping the mass equally at the nodes whereupon the integral over the body is reduced to a sum over nodes. The nonlinear system is solved by Newton-Raphson iteration.

§R.23. Linear Triangle Best Fit

Consider a constant thickness three-node linear plane stress triangle (also known as Turner triangle and CST), displacing in two dimensions as illustrated in Figure R.6. To facilitate node subscripting, rename $X_1 \to X$, $X_2 \to Y$, $x_1 \to x$, $x_2 \to y$, $u_1 \to u_x$, $u_2 \to u_y$. Using triangular coordinates $\{\zeta_1, \zeta_2, \zeta_3\}$ position coordinates and displacements are interpolated linearly: $X = X_1\zeta_1 + X_2\zeta_2 + X_3\zeta_3$, $Y = Y_1\zeta_1 + Y_2\zeta_2 + Y_3\zeta_3$, $x = x_1\zeta_1 + x_2\zeta_2 + x_3\zeta_3$, $y = y_1\zeta_1 + y_2\zeta_2 + y_3\zeta_3$, $u_x = u_{y1}\zeta_1 + u_{x2}\zeta_2 + u_{x3}\zeta_3$ and $u_y = u_{y1}\zeta_1 + u_{y2}\zeta_2 + u_{y3}\zeta_3$, in which numerical subscripts now denote node numbers. Insert into (R.73) and introduce side conditions $X_1 + = X_2 + X_3 = 0$, $Y_1 + Y_2 + Y_3 = 0$, $u_{x1} + u_{x2} + u_{x3} = x_1 + x_2 + x_3$ and $u_{y1} + u_{y2} + u_{y3} = y_1 + y_2 + y_3$ for centroid positioning. *Mathematica* found for the best fit angle

$$\tan\theta_3 = \frac{x_1 Y_1 + x_2 Y_2 + x_3 Y_3 - y_1 X_1 - y_2 X_2 - y_3 X_3}{x_1 X_1 + x_2 X_2 + x_3 X_3 + y_1 Y_1 + y_2 Y_2 + y_3 Y_3}. \tag{R.74}$$

where $x_a = x_a + u_{xa}$, $y_a = y_a + u_{ya}$, $a = 1, 2, 3$. The same result can be obtained with any 3-point integration rule where the Gauss points are placed on the medians. In particular, Rankin's idea of using the three corners as integration points [R.67] gives the same answer.

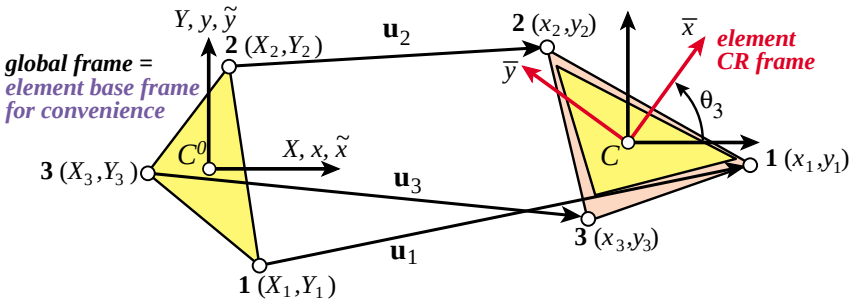

FIGURE R.6. Best CR frame fit to 3-node linear triangle in 2D. Axes relabeled as explained in the text.

This solution is interesting in that it can be used as an approximation for any 3-node triangle undergoing three dimensional motion (for example, a thin shell facet element) as long as axis $\bar{x}_3$ is preset normal to the plane passing through the three deformed corners. The assumption is that the best fit is done only for the in-plane displacements.

§R.24. Rigid Body Motion Verification

Suppose the element motion $\mathbf{u} = \mathbf{u}_r$ is rigid ($\mathbf{u}_d = \mathbf{0}$) with rotator $\mathbf{R}_r$. If so $\mathbf{u}_r = \mathbf{c} - (\mathbf{I} - \mathbf{R}_r)\mathbf{X}$. Inserting into (R.68) yields

$$J = \tfrac{1}{2}\int \mathbf{X}^T(\mathbf{R}_r - \mathbf{R}_0)^T(\mathbf{R}_r - \mathbf{R}_0)\mathbf{X}\; dV. \tag{R.75}$$

in which $\mathbf{X} = \mathbf{x}^G - \mathbf{a}$. This is clearly minimized by $\mathbf{R}_0 = \mathbf{R}_r$, so the body attached frame is a best fit CR frame. (There may be additional solutions if $(\mathbf{R}_r - \mathbf{R}_0)\mathbf{X} \equiv \mathbf{0}$ for some $\mathbf{R}_0 \neq \mathbf{R}_r$, for example by relabeling axes.) This check verifies that the functional (R.68) also works as expected for rigid body components of a structural model.

§R.25. Nomenclature

The notation used by different investigators working in CR formulations has not coalesced, since the topic is in flux. This Appendix identifies the symbols used in the present article. General scheme of notation is

Non-bold letters: scalars. Uppercase bold letters (roman and greek): matrices and tensors. Lowercase bold letters (roman and greek): column vectors, but there are occasional exceptions such as **X** and **Y**.

Symbol	*Meaning*
a	As subscript: generic nodal index
b	As subscript: generic nodal index
b_i	Components of Rodrigues-Cayley axial vector.
c_i	Generic coefficients. Components of vector **c**.
d	As subscript: deformational
e	Base of natural logarithms. As superscript: element index.
e_{ij}	Strains.
f_i	Components of force vector **f**
h_i	Triangle heights.
i	As subscript: generic index. Imaginary unit in complex numbers.
j	As subscript: generic index
k	As superscript: iteration count
l	As subscript: generic index
m	As subscript: generic index
n	As subscript: incremental step number
n_i	Components of vector **n**.
p_i	Quaternion components.
r	As subscript: rigid
s_{kx}, s_{ky}	Projections of triangle side L_k on $\{x, y\}$ axes.
t	Time.
u	Displacement magnitude
u_i, $\tilde{u}_i$, $\bar{u}_i$	Displacement components in x_i, $\tilde{x}_i$, $\bar{x}_i$ axes, respectively.
u_{di}, $\tilde{u}_{di}$, $\bar{u}_{di}$	Deformational displacement components in x_i, $\tilde{x}_i$, $\bar{x}_i$ axes, respectively.
u_{ri}, $\tilde{u}_{ri}$, $\bar{u}_{ri}$	Rigid displacement components in x_i, $\tilde{x}_i$, $\bar{x}_i$ axes, respectively.
x	x_1 axis when using $\{x, y, z\}$ notation
x_i	Components of global-frame position vector **x**
$\tilde{x}_i$	Components of element base-frame position vector $\tilde{\mathbf{x}}$.
$\bar{x}_i$	Components of element CR-frame position vector $\bar{\mathbf{x}}$.
y	x_2 axis when using $\{x, y, z\}$ notation
z	x_3 axis when using $\{x, y, z\}$ notation
A	Area.
C	Generic centroid of body or element in statics. Center of mass in dynamics.
C^0,C^R,C	Body or element centroid in base, CR and deformed configurations, respectively.
L	Length of 2-node element. Generic length.
L_k	Length of triangle side opposite node k.
N	Number of structure nodes.
N^e	Number of nodes of element e.
O	Origin of global frame.
T	Kinetic energy
U	Internal energy, strain energy.
W	External work.
X	x_1 axis when using $\{X, Y, Z\}$ notation
X_i	Material global Cartesian axes
Y	x_2 axis when using $\{X, Y, Z\}$ notation
Z	x_3 axis when using $\{X, Y, Z\}$ notation

$\mathbf{a}$	Position vector of C^0 from origin of global frame. Generic vector.
$\mathbf{b}$	Position vector of $C^R \equiv C$ from origin of global frame. Generic vector.
$\mathbf{c}$	Displacement of base element centroid C^0 to $C^R \equiv C$.
$\mathbf{d}$	Deformational displacement. Array of nodal DOF, collecting translations and rotations.
$\bar{\mathbf{d}}$	Array of nodal deformational DOF, collecting translations and rotations.
$\mathbf{e}$	Strains arranged as vector.
$\mathbf{f}$	Generic force vector. External force vector.
$\bar{\mathbf{f}}$	External force vector in element CR frame.
$\mathbf{f}_b$	Balance (self-equilibrated) force vector.
$\mathbf{f}_u$	Unbalanced (out of equilibrium) force vector.
$\mathbf{i}$	Base unit vector
$\mathbf{m}$	Generic nodal moment vector.
$\mathbf{m}_a$	Nodal moment components at node a.
$\mathbf{n}$	Unit normal. Direction of rotation vector in 3D.
$\mathbf{n}_a$	Translational force components at node a.
$\mathbf{0}$	Null matrix or vector.
$\mathbf{p}$	Internal force vector of structure.
$\mathbf{p}^e$	Element internal force vector in global frame.
$\bar{\mathbf{p}}^e$	Element internal force vector in CR frame.
$\mathbf{q}$	Not used
$\mathbf{r}$	Force residual vector.
$\mathbf{u}$	Displacement vector. Also generic vector: meaning from context.
$\mathbf{v}$	Denotes vector collecting nodal displacements and rotations, displacements and spins, or displacements and rotators. See Table R.2. Also generic vector: meaning from context.
$\mathbf{w}$	Generic vector: meaning from context.
$\hat{\mathbf{v}}$	Global DOF vector for complete structure.
$\mathbf{x}$	Global-frame spatial position vector.
$\tilde{\mathbf{x}}$	Element base-frame position vector.
$\bar{\mathbf{x}}$	Element CR-frame position vector.
$\vec{\mathbf{x}}$	Frame independent position vector.
$\mathbf{y}$	Alternative notation for position vector. Generic vector.
$\vec{\mathbf{y}}$	Frame independent position vector.
$\mathbf{z}_i$	Spinor eigenvector.
$\mathbf{A}$	Generic matrix.
$\mathbf{B}_d$	Matrix relating strains to deformational displacements. Generic matrix.
$\mathbf{C}$	Strain-stress (compliance) matrix
$\mathbf{D}$	Diagonal matrix of zeros and ones. Generic diagonal matrix, size from context.
$\mathbf{E}$	Stress-strain (elasticity) matrix
$\mathbf{F}$	Generic matrix function
$\mathbf{F}_n$, $\mathbf{F}_{nm}$	Auxiliary matrices in tangent stiffness derivations.
$\mathbf{G}$	Element spin-fitter matrix linking $\delta\boldsymbol{\omega}_r^e$ to $\delta\mathbf{v}^e$.
$\mathbf{G}_a$	Component of $\mathbf{G}$ associated with node a.
$\mathbf{H}$	Block diagonal matrix built with $\mathbf{H}_a$ and $\mathbf{I}$ blocks.
$\mathbf{H}_a$	Evaluation of $\mathbf{H}(\boldsymbol{\theta})$ at node a.
$\mathbf{H}(\boldsymbol{\theta})$	Jacobian of $\boldsymbol{\theta}$ with respect to $\boldsymbol{\omega}$.
$\mathbf{I}$	Identity matrix, size from context.
$\mathbf{J}$	Jacobian matrix in general.
$\mathbf{J}_{ab}$	Jacobian matrix relating quantities at nodes a and b.
$\mathbf{K}$	Tangent stiffness matrix of structure.
$\mathbf{K}^e$	Element tangent stiffness matrix in global frame.
$\bar{\mathbf{K}}^e$	Linear element stiffness matrix in local CR frame.

$\bar{\mathbf{K}}_R^e$	Element tangent stiffness matrix in local CR frame.
$\mathbf{K}_{GM}$	Moment correction geometric stiffness matrix.
$\mathbf{K}_{GP}$	Equilibrium projection geometric stiffness matrix.
$\mathbf{K}_{GR}$	Rotational geometric stiffness matrix.
$\mathbf{K}_M$	Material stiffness matrix.
$\mathbf{L}$	Block diagonal built with $\mathbf{L}_a$ and $\mathbf{0}$ blocks.
$\mathbf{L}_a$	Evaluation of $\mathbf{L}(\boldsymbol{\theta}, \mathbf{m})$ at node a.
$\mathbf{L}(\boldsymbol{\theta}, \mathbf{m})$	Contraction of $\partial \mathbf{H}(\boldsymbol{\theta})^T / \partial \boldsymbol{\omega})$ with vector $\mathbf{m}$
$\mathbf{M}$	Mass matrix.
$\mathbf{N}$	Spinor for vector $\mathbf{n}$.
$\mathbf{P}$	Projector matrix.
$\mathbf{P}_u$	Translational projector matrix, a.k.a. T-projector.
$\mathbf{P}_\omega$	Rotational projector matrix, a.k.a. R-projector.
$\mathbf{Q}$	Generic orthogonal matrix.
$\mathbf{R}$	Orthogonal rotation matrix: the matrix representation of a rotator.
$\mathbf{R}_0$	Transformation rotator between element base frame and CR frame.
$\tilde{\mathbf{R}}_0$, $\bar{\mathbf{R}}_0$	Rotator $\mathbf{R}_0$ referred to element base and CR frames, respectively.
$\mathbf{S}$	Spin-lever (a.k.a. moment-arm) matrix built up of $\mathbf{S}_a$ blocks. Generic skew-symmetric matrix.
$\mathbf{S}_a$	Spin-lever matrix for node a.
$\mathbf{T}$	Element CR-to-global transformation matrix built from $\mathbf{T}_R$ blocks.
$\mathbf{T}_0$	Transformation rotator from element base frame to global frame.
$\mathbf{T}_R$	Transformation rotator from element CR frame to global frame.
$\mathbf{U}_{ab}$	Building block of translational projector $\mathbf{P}_u$.
$\mathbf{V}$	Generic skew-symmetric matrix.
$\mathbf{W}$	Generic skew-symmetric matrix.
$\mathbf{X}$	Global position vector with X_i as components.
$\bar{\bar{\mathbf{X}}}$	Coordinate free material position vector.
$\tilde{\mathbf{X}}$	Element base position vector with$\tilde{x}_i$ as components.
$\bar{\mathbf{X}}$	Element CR position vector with $\bar{x}_i$ as components.
$\mathbf{Y}$	Position vector collecting y_i as components.
$\mathbf{Z}$	Matrix of right eigenvectors of spinor.
α	Coefficient in parametrized rotator representation.
β	Coefficient in parametrized rotator representation.
γ	Spinor normalization factor.
δ	Variation symbol.
δ_{ab}	Kronecker delta.
ϵ	Small scalar
ζ_i	Triangular coordinates
η	Coefficient in $\mathbf{H}(\boldsymbol{\theta})$.
θ	Rotation angle in general. Magnitude of rotation vector $\boldsymbol{\theta}$.
κ	Curvature
λ	Lagrange multiplier
μ	Coefficient in $\mathbf{L}(\boldsymbol{\theta}, \mathbf{m})$.
ν	Poisson's ratio
ρ	Mass density.
σ_{ij}	Stresses.
τ	Coefficient in $\mathbf{Log}_e(\mathbf{R})$ formula.
χ,ϕ,φ,ψ	Generic angle symbols.
ψ	Generic angle.
ω	Magnitude of spin vector $\boldsymbol{\omega}$.
Σ	Summation symbol.
Σ_a, Σ_b	Abbreviations for $\sum_{a=1}^{N^e}$ and $\sum_{b=1}^{N^e}$.

$\boldsymbol{\theta}$	Rotation axial vector (a.k.a. rotation pseudovector).
$\boldsymbol{\phi}$	Axial vector built from ϕ_i angles.
$\boldsymbol{\psi}$	Axial vector built from ψ_i angles.
$\boldsymbol{\sigma}$	Stresses arranged as vector.
$\boldsymbol{\sigma}_0$	Initial stresses (in the base configuration) arranged as vector.
$\boldsymbol{\omega}$	Spin axial vector (a.k.a. spin pseudovector).
$\mathbf{\Gamma}$	Auxiliary matrix used in the decomposition of $\mathbf{G}$
$\mathbf{\Theta}$	Spinor built from rotation axial vector.
$\mathbf{\Lambda}$	Diagonal matrix of eigenvalues of $\mathbf{\Omega}$.
$\mathbf{\Xi}$	Auxiliary matrix used in the decomposition of $\mathbf{G}$.
$\mathbf{\Phi}$	Spinor built from axial vector $\boldsymbol{\phi}$.
$\mathbf{\Psi}$	Spinor built from axial vector $\boldsymbol{\psi}$.
$\boldsymbol{\Sigma}$	Spinor built from the Rodrigues-Cayley parameters b_i.
$\mathbf{\Omega}$	Spinor built from spin axial vector $\boldsymbol{\omega}$.
$\mathbf{\Omega}_p$	Spinor build from quaternion parameters p_i.
$\mathcal{C}$	Configuration: see Table R.1 for further identification by superscripts.
CR	Abbreviation for corotational (a.k.a. corotated) kinematic description.
DOF	Abbreviation for degree of freedom.
EICR	Abbreviation for Element Independent Corotational formulation.
Rotator	Abbreviation for rotation tensor (or 3×3 rotation matrix).
Spinor	Abbreviation for spin tensor (or 3×3 spin matrix).
TL	Abbreviation for Total Lagrangian kinematic description.
UL	Abbreviation for Updated Lagrangian kinematic description.
$\dot{(.)}$	Abbreviation for $d(.)/dt$
$(.)^0$ or $(.)_0$	$(.)$ pertains to base (initial) configuration $\mathcal{C}^0$.
$(.)^D$ or $(.)_D$	$(.)$ pertains to deformed configuration $\mathcal{C}^D$.
$(.)^G$ or $(.)_G$	$(.)$ pertains to globally aligned configuration $\mathcal{C}^G$.
$(.)^R$ or $(.)_R$	$(.)$ pertains to corotated configuration $\mathcal{C}^R$.
$(.)_d$	$(.)$ is deformational.
$(.)^e$	$(.)$ pertains to element e.
$(.)_r$	$(.)$ is rigid.
$()^T$	Matrix or vector transposition.
$()^{-1}$	Matrix inverse.
axial(.)	Extraction of axial vector from skew-symmetric matrix argument
$e^{(.)}$	Matrix exponential if $(.)$ is a square matrix
Exp(.)	Alternative form for matrix exponential
$\mathbf{Log}_e(.)$	Matrix natural logarithm
Rot(.)	Construction of rotator from spinor argument
Skew(.)	Extraction of spinor from rotator argument
Spin(.)	Construction of spinor from axial vector argument
trace(.)	Sum of diagonal entries of matrix argument

References

[R.1] J. H. Argyris, An excursion into large rotations, *Comp. Meths. Appl. Mech. Engrg.*, **32**, 85–155, 1982.

[R.2] J.-M. Battini, C. Pacoste, Co-rotational beam elements with warping effects in instability problems, *Comp. Meths. Appl. Mech. Engrg.*, **191**, 1755–1789, 2002.

[R.3] J.-M. Battini, C. Pacoste, Plastic instability of beam structures using co-rotational elements, *Comp. Meths. Appl. Mech. Engrg.*, **191**, 5811–5831, 2002.

[R.4] K.-J. Bathe, *Finite Element Procedures in Engineering Analysis*, Prentice-Hall, 1982.

[R.5] K.-J. Bathe, E. Ramm and E. L. Wilson, Finite element formulations for large deformation dynamic analysis, *Int. J. Numer. Meth. Engrg.*, **7**, 255–271, 1973.

[R.6] R. Bellman, *Introduction to Matrix Analysis*, McGraw-Hill, New York, 1960.

[R.7] T. Belytschko and B. J. Hsieh, Nonlinear transient finite element analysis with convected coordinates, *Int. J. Numer. Meth. Engrg.*, **7**, 255-271, 1973.

[R.8] T. Belytschko and B. J. Hsieh, Application of higher order corotational stretch theories to nonlinear finite element analysis, *Computers & Structures*, **11**, 175–182, 1979.

[R.9] T. Belytschko and B. J. Hsieh, An overview of semidiscretization and time integration operators, Chapter 1 in *Computational Methods for Transient Analysis*, T. Belytschko and T. J. R. Hughes, (eds.), North-Holland, Amsterdam, 1–66, 1983.

[R.10] P. G. Bergan and G. Horrigmoe, Incremental variational principles and finite element models for nonlinear problems, *Comp. Meths. Appl. Mech. Engrg.*, **7**, 201–217, 1976.

[R.11] P. G. Bergan and L. Hanssen, A new approach for deriving 'good' finite elements, MAFELAP II Conference, Brunel University, 1975, in *The Mathematics of Finite Elements and Applications – Volume II*, ed. by J. R. Whiteman, Academic Press, London, 483–497, 1976.

[R.12] P. G. Bergan, Finite elements based on energy orthogonal functions, *Int. J. Numer. Meth. Engrg.*, **15**, 1141–1555, 1980.

[R.13] P. G. Bergan and M. K. Nygård, Finite elements with increased freedom in choosing shape functions, *Int. J. Numer. Meth. Engrg.*, **20**, 643–664, 1984.

[R.14] P. G. Bergan and C. A. Felippa, A triangular membrane element with rotational degrees of freedom, *Comp. Meths. Appl. Mech. Engrg.*, **50**, 25–69, 1985.

[R.15] P. G. Bergan and M. K. Nygård, Nonlinear shell analysis using Free Formulation finite elements, in *Finite Element Methods for Nonlinear Problems*, Springer Verlag, Berlin, 317-338, 1989.

[R.16] M. A. Biot, *The Mechanics of Incremental Deformations*, McGraw-Hill, New York, 1965.

[R.17] R. B. Bird, R. C. Amstrong and O. Hassager, *Dynamics of Polymeric Liquids. Vol 1: Fluid Dynamics*, Wiley, New York, 1977.

[R.18] R. O. Bjærum, Finite element formulations and solution algorithms for buckling and collapse analysis of thin shells. *Dr. Ing. Thesis*, Div. of Structural Mechanics, Norwegian Institute of Technology, Trondheim, Norway, 1992.

[R.19] A. Cayley, *Collected Works*, Cambridge Univ. Press, 1898.

[R.20] H. Cheng and K. C. Gupta, An historical note on finite rotations, *J. Appl. Mech.*, **56**, 139–145, 1989.

[R.21] M. Chiesa, B. Skallerud and D. Gross, Closed form line spring yield surfaces for deep and shallow cracks: formulation and numerical performance, *Computers & Structures*, **80**, 533–545, 2002.

[R.22] M. A. Crisfield, A consistent corotational formulation for nonlinear three-dimensional beam element, *Comp. Meths. Appl. Mech. Engrg.*, **81**, 131–150, 1990.

[R.23] M. A. Crisfield and G. F. Moita, A unified co-rotational for solids, shells and beams, *Int. J. Solids Struc.*, **33**, 2969–2992, 1996.

[R.24] M. A. Crisfield, *Nonlinear Finite Element Analysis of Solids and Structures. Vol 2: Advanced Topics*, Wiley, Chichester, 1997.

[R.25] B. M. Fraeijs de Veubeke, The dynamics of flexible bodies, *Int. J. Engrg. Sci.*, **14**, 895-913, 1976.

[R.26] C. Farhat, P. Geuzaine and G. Brown, Application of a three-field nonlinear fluid-structure formulation to the prediction of the aeroelastic parameters of an F-16 fighter, *Computers and Fluids*, **32**, 3–29, 2003.

[R.27] C. A. Felippa and C. Militello, Membrane triangles with corner drilling freedoms: II. The ANDES element, *Finite Elem. Anal. Des.*, **12**, 189–201, 1992.

[R.28] C. A. Felippa and S. Alexander, Membrane triangles with corner drilling freedoms: III. Implementation and performance evaluation, *Finite Elem. Anal. Des.*, **12**, 203–239, 1992.

[R.29] C. A. Felippa, A systematic approach to the Element-Independent Corotational dynamics of finite elements. Report CU-CAS-00-03, Center for Aerospace Structures, College of Engineering and Applied Sciences, University of Colorado at Boulder, January 2000.

[R.30] C. A. Felippa and K. C. Park, The construction of free-free flexibility matrices for multilevel structural analysis, *Comp. Meths. Appl. Mech. Engrg.*, **191**, 2111–2140, 2002.

[R.31] C. A. Felippa, Recent advances in finite element templates, Chapter 4 in *Computational Mechanics for the Twenty-First Century*, ed. by B.H.V. Topping, Saxe-Coburn Publications, Edinburgh, 71–98, 2000.

[R.32] C. A. Felippa, A study of optimal membrane triangles with drilling freedoms, *Comp. Meths. Appl. Mech. Engrg.*, **192**, 2125–2168, 2003.

[R.33] F. R. Gantmacher, *The Theory of Matrices*, Vol. I, Chelsea, New York, 1960.

[R.34] M. Geradin, Finite element approach to kinematic and dynamic analysis of mechanisms using Euler parameters, in *Numerical Methods for Nonlinear Problems II*, ed. by C. Taylor, E. Hinton and D. R. J. Owen, Pineridge Press, Swansea, 1984.

[R.35] H. Goldstein, *Classical Mechanics*, Addison-Wesley, Reading, Massachussets, 1950.

[R.36] M. Hammermesh, *Group Theory and Its Application to Physical Problems*, Dover, New York, 1989.

[R.37] B. Haugen, Buckling and stability problems for thin shell structures using high-performance finite elements, *Ph. D. Dissertation*, Dept. of Aerospace Engineering Sciences, University of Colorado, Boulder, CO, 1994.

[R.38] B. Haugen and C. A. Felippa, A unified formulation of small-strain corotational finite elements: II. Applications to shells and mechanisms, in preparation.

[R.39] G. Horrigmoe, Finite element instability analysis of free-form shells, *Dr. Ing. Thesis*, Div. of Structural Mechanics, Norwegian Institute of Technology, Trondheim, Norway, 1977.

[R.40] G. Horrigmoe and P. G. Bergan, Instability analysis of free-form shells by flat finite elements, *Comp. Meths. Appl. Mech. Engrg.*, **16**, 11–35, 1978.

[R.41] A. S. Householder, *The Theory of Matrices in Numerical Analysis*, Blaisdell, New York, 1964.

[R.42] T. J. R. Hughes and W.-K. Liu, Nonlinear finite element analysis of shells: Part I. Three-dimensional shells, *Comp. Meths. Appl. Mech. Engrg.*, **26**, 331–362, 1981.

[R.43] T. J. R. Hughes and W.-K. Liu, Nonlinear finite element analysis of shells: Part II. Two-dimensional shells, *Comp. Meths. Appl. Mech. Engrg.*, **27**, 167–182, 1981.

[R.44] T. J. R. Hughes and J. Winget, Finite rotation effects in numerical integration of rate constitutive equations arising in large deformation analysis, *Int. J. Numer. Meth. Engrg.*, **15**, 1862–1867, 1980.

[R.45] B. M. Irons and S. Ahmad, *Techniques of Finite Elements*, Ellis Horwood Ltd, 1980.

[R.46] B. Kråkeland, Large displacement analysis of shells considering elastoplastic and elastoviscoplastic materials, *Dr. Ing. Thesis*, Div. of Structural Mechanics, Norwegian Institute of Technology, Trondheim, Norway, 1977.

[R.47] E. Levold, Solid mechanics and material models including large deformations, *Dr. Ing. Thesis*, Div. of Structural Mechanics, Norwegian Institute of Technology, Trondheim, Norway, 1990.

[R.48] K. M. Mathisen, Large displacement analysis of flexible and rigid systems considering displacement-dependent loads and nonlinear constraints. *Dr. Ing. Thesis*, Div. of Structural Mechanics, Norwegian Institute of Technology, Trondheim, Norway, 1990.

[R.49] K. M. Mathisen, T. Kvamsdal and K. M. Okstad, Adaptive strategies for nonlinear finite element analysis of shell structures, In: *Numerical Methods in Engineering '92*, C. Hirchs et al. (Eds.), Elsevier Science Publishers B. V., 1992.

[R.50] K. Mattiasson, On the corotational finite element formulation for large deformation problems, *Dr. Ing. Thesis*, Dept. of Structural Mechanics, Chalmers University of Technology, Göteborg, 1983.

[R.51] K. Mattiasson and A. Samuelsson, Total and updated Lagrangian forms of the co-rotational finite element formulation in geometrically and materially nonlinear analysis, in *Numerical Methods for Nonlinear Problems II*, ed. by C. Taylor, E. Hinton and D. R. J. Owen, Pineridge Press, Swansea, 134–151, 1984.

[R.52] K. Mattiasson, A. Bengston and A. Samuelsson, On the accuracy and efficiency of numerical algorithms for geometrically nonlinear structural analysis, in *Finite Element Methods for Nonlinear Problems*, ed. by P. G. Bergan, K. J. Bathe and W. Wunderlich, Springer-Verlag, 3–23, 1986.

[R.53] C. Militello and C. A. Felippa, The first ANDES elements: 9-DOF plate bending triangles, *Comp. Meths. Appl. Mech. Engrg.*, **93**, 217–246, 1991.

[R.54] B. Nour-Omid and C. C. Rankin, Finite rotation analysis and consistent linearization using projectors, *Comp. Meths. Appl. Mech. Engrg.*, **93**, 353–384, 1991.

[R.55] V. V. Novozhilov, *Foundations of the Nonlinear Theory of Elasticity*, Graylock Press, Rochester, 1953.

[R.56] M. K. Nygård and P. G. Bergan, Advances in treating large rotations for nonlinear problems, Chapter 10 in *State-of the Art Surveys on Computational Mechanics*, ed. by A. K. Noor and J. T. Oden, ASME, New York, 305–332, 1989.

[R.57] M. K. Nygård, Large displacement analysis of flexible and rigid systems considering displacement-dependent loads and nonlinear constraints. *Dr. Ing. Thesis*, Div. of Structural Mechanics, Norwegian Institute of Technology, Trondheim, Norway, 1990.

[R.58] C. Pacoste, Co-rotational flat facet triangular elements for shell instability analysis, *Comp. Meths. Appl. Mech. Engrg.*, **156**, 75-110, 1998.

[R.59] K. C. Park and G. M. Stanley, A curved C^0 shell element based on assumed natural-coordinate strains, *J. Appl. Mech.*, **53**, 278–290, 1986.

[R.60] W. Pietraszkiewicz, Finite rotations in shells, in *Theory of Shells, Proc. 3rd IUTAM Symp on Shell Theory, Tsibili 1978*, 445–471, North Holland, Amsterdam, 1980.

[R.61] W. Pietraszkiewicz (ed.), *Finite Rotations in Structural Mechanics*, Lecture Notes in Engineering 19, Springer-Verlag, Berlin, 1985.

[R.62] E. Ramm, A plate/shell element for large deflections and rotations, *Proc. US-Germany Symposium on Formulations and Algorithms in Finite Element Analysis*, MIT-Cambridge, Mass., 264–293, 1976.

[R.63] C. C. Rankin and F.A. Brogan, An element-independent corotational procedure for the treatment of large rotations, *ASME J. Pressure Vessel Technology*, **108**, 165–174, 1986.

[R.64] C. C. Rankin, Consistent linearization of the element-independent corotational formulation for the structural analysis of general shells, *NASA Contractor Report 278428*, Lockheed Palo Alto Res. Lab., CA, 1988.

[R.65] C. C. Rankin and B. Nour-Omid, The use of projectors to improve finite element performance, *Computers & Structures*, **30**, 257–267, 1988.

[R.66] C. C. Rankin, Consistent linearization of the element-independent corotational formulation for the structural analysis of general shells, *NASA Contractor Report 278428*, Lockheed Palo Alto Research Laboratory, Palo Alto, CA, 1988.

[R.67] C. C. Rankin, On choice of best possible corotational element frame, in *Modeling and Simulation Based Engineering*, ed by S. N. Atluri and P. E. O'Donoghue, Tech Science Press, Palmdale, CA, 1998.

[R.68] C. C. Rankin, F. A. Brogan, W. A. Loden and H. Cabiness, *STAGS User Manual*, LMMS P032594, Version 3.0, January 1998.

[R.69] O. Rodrigues, Des lois géometriques qui regissent les déplacements d'un systéme solide dans l'espace, et de la variation des coordonnées provenant de ces déplacement considerées indépendent des causes qui peuvent les produire, *J. de Mathématiques Pures et Appliquées*, **5**, 380–400, 1840.

[R.70] J. G. Simmonds and D. A. Danielson, Nonlinear shell theory with finite rotation and stress function vectors, *J. Appl. Mech.*, **39**, 1085–1090, 1972.

[R.71] J. C. Simo, A finite strain beam formulation. Part I: The three-dimensional dynamic problem, *Comp. Meths. Appl. Mech. Engrg.*, **49**, 55–70, 1985.

[R.72] J. C. Simo and L. Vu-Quoc, A finite strain beam formulation. Part II: Computational aspects, *Comp. Meths. Appl. Mech. Engrg.*, **58**, 79–116, 1986.

[R.73] O. I. Sivertsen, *Virtual Testing of Mechanical Systems: Theories and Techniques*, Swets & Zeitlinger Pubs., Heereweg, Netherlands, 2001.

[R.74] B. Skallerud and B. Haugen, Collapse of thin shell structures: Stress resultant plasticity modeling within a co-rotated ANDES finite element formulation, *Int. J. Numer. Meth. Engrg.*, **46**, 1961–1986, 1999.

[R.75] B. Skallerud, K. Holthe and B. Haugen, Combining haigh-performance thin shell and surface crack finite elements for simulation of combined failure modes, *Proc. 7^{th} US Nat. Congress in Computational Mechanics*, Albuquerque, NM, July 2003.

[R.76] R. A. Spurrier, A comment on singularity-free extraction of a quaternion from a direction cosine matrix, *J. Spacecrafts & Rockets*, **15**, p. 255, 1978.

[R.77] M. L. Szwabowicz, Variational Formulation in the Geometrically Nonlinear Thin Elastic Shell Theory, *Int. J. Solids Struc.*, **22**, 1161–1175, 1986.

[R.78] R. Tanner, *Engineering Rheology*, Oxford University Press, 1985.

[R.79] J. G. Teigen, Nonlinear analysis of concrete structures based on a 3D shear-beam element formulation. *Ph.D Dissertation*, Department of Mathematics, Mechanics Division, University of Oslo, Oslo, Norway, 1994.

[R.80] C. Truesdell, *Continuum Mechanics I: The Mechanical Foundations of Elasticity and Fluid Dynamics*, Gordon & Breach, New York, 1966; corrected reprint of *ibid*., J. Rational Mech. Anal., **1**, 125–300, 1952.

[R.81] C. Truesdell and R. A. Toupin. The classical field theories, in S. Flügge, editor, *Handbuch der Physik*, vol. III/1, 226–790, Springer Verlag, Berlin, 1960.

[R.82] C. Truesdell, Hypoelasticity, *J. Rational Mech.*, **4**, 83–133, 1019–1020, 1955. Reprinted in *Foundations of Elasticity Theory*, Gordon & Breach, New York, 1965.

[R.83] C. Truesdell and W. Noll, The Nonlinear Field theories of Mechanics, in in S. Flügge, editor, *Handbuch der Physik*, Vol. III/3, Springer-Verlag, 1965.

[R.84] H. W. Turnbull, *The Theory of Determinants, Matrices and Invariants*, Blackie and Son, London, 1929.

[R.85] K. C. Valanis, A theory of viscoplasticity without a yield surface, Part II: Application to mechanical behavior of metals, Arch. Mech., **23**, 535–551, 1971.

[R.86] G. A. Wempner, Finite elements, finite rotations and small strains of flexible shells, *Int. J. Solids Struc.*, Vol 5, 117–153, 1969